ADVANCES IN INORGANIC CHEMISTRY, VOL. 45

THE METHYLAMINE DEHYDROGENASE ELECTRON TRANSFER CHAIN

C. DENNISON,*[,1] G. W. CANTERS,* S. DE VRIES,† E. VIJGENBOOM,* and R. J. VAN SPANNING‡

*Leiden Institute of Chemistry, Gorlaeus Laboratories, Leiden University, 2300 RA Leiden, The Netherlands
†Laboratory for Microbiology and Enzymology, Technical University of Delft, 2628 BC Delft, The Netherlands
‡Biological Laboratory, Free University of Amsterdam, 1007 MC Amsterdam, The Netherlands

I. Introduction

Textbook coverage of cellular respiration is often based on the mitochondrial paradigm. Mitochondiral respiration is attractive because of its relatively uncomplicated organization. The respiratory chain consists of a single sequence of redox proteins with only two possible substrates and a single terminal electron acceptor. The simplicity of the mitochondrial respiratory apparatus belies its evolutionary origin.

[1] Present address: Department of Chemistry, University College Dublin, Belfield, Dublin 4, Ireland.

0898-8838/98 $25.00

According to the endosymbiontic hypothesis mitochondria derive from ancestors that are closely related to modern purple bacteria, for example, *Pseudomonas, Rhodobacter,* and *Paracoccus.* Although mitochondria are embedded in a cellular environment with narrowly controlled conditions regarding pH, redox balance, and substrate availability, bacteria may encounter a variety of environmental conditions. A repertoire of respiratory chains and regulatory mechanisms as opposed to a single electron transfer chain allows them to cope with a variety of environments.

During respiration cellular redox free energy is converted into chemic-osmotic and chemical energy. The conversion is mediated by the flow of electrons, which, in an oxidizing environment, run from low to high potential. In mitochondria the reducing equivalents flow via NADH and ubiquinone to the terminal electron acceptor, molecular oxygen. In bacteria the reducing equivalents may be derived from a variety of sources, such as sulfur or nitrogen in low oxidation states (S, S^{2-}, NH_3), molecular hydrogen, or even ferrous ions. Terminal electron acceptors may by provided by molecular oxygen, or by sulfur and nitrogen in high oxidation states, e.g., SO_4^{2-}, NO_2^-, and NO_3^-. A bacterium has a collection of respiratory routes at its disposal, thus unraveling the respiratory machinery is a complicated task requiring not only identification of branches of the various electron transport chains and their composition, but also the elucidation of their genetic organization and the mechanisms that control selective gene activation and expression.

This review focuses on the electron transfer chain that is employed by the organism *Paracoccus versutus* [formerly *Thiobacillus versutus* (*1*)] when it is provided with methylamine as its sole source of nitrogen and energy. The chain is similar to the methylamine dehydrogenase chain of *Paracoccus denitrificans*, and the results of the *P. versutus* studies will be compared with the *P. denitrificans* data where appropriate. One of the attractive features of this chain is that it consists of only four redox components: methylamine dehydrogenase (MADH), amicyanin (ami), cytochrome c_{550}, and cytochrome *c* oxidase (COX). Only MADH contains an organic prosthetic group, tryptophan-tryptophyl quinone (TTQ); the other three proteins contain metals (Fe and Cu) as their prosthetic group. MADH converts methylamine to formaldehyde and ammonia, which then enter the metabolic cycles of the cell, while the electrons that are liberated in the conversion step are fed into amicyanin and, subsequently via cyt c_{550}, into COX, where they are used for the reduction of the terminal electron acceptor, molecular oxygen, to water.

In Section II the composition and organisation of the respiratory chains of *P. versutus* and *P. denitrificans* will be reviewed. The gene organization and composition, and their possible control elements, will also be discussed. Section III will deal with the structure and function of the four components of the MADH redox chain. Structures determined by X-ray diffraction (XRD) and nuclear magnetic resonance (NMR) techniques are available for the members of the MADH chain or for closely related analogues. Finally, the enzymology and reaction kinetics of the chain will be reviewed.

II. Composition and Organization of Respiratory Chains

A. The Respiratory Network of *Paracoccus versutus* and *Paracoccus denitrificans*

1. Introduction

Paracoccus versutus and *P. denitrificans* (*2*) are phylogenetically closely related species; together with *Rhodobacter* and *Rhizobium* species they belong to the α-cluster of purple bacteria (*3*, *4*). These gram-negative eubacteria are unable to ferment availabe growth substrates, and are therefore completely dependent on respiration-linked oxidative phosphorylation for their (free) energy requirements. Usually, these organisms are found in soil, sewage, or sludge, environments where the availability of suitable carbon and energy sources as well as of terminal electron acceptors is subject to ever-fluctuating conditions. The ability of the cells to survive in these variable environments depends on the properties of their respiratory network as well as on their readiness to adapt to environmental changes.

One of the best studied organisms in this respect is *P. denitrificans* (*5*, *6*, *7*, *8*). This bacterium has a great nutritional adaptability: it can grow chemolithoautotrophically with hydrogen or thiosulfate as sole energy source; autotrophically with methanol, formaldehyde, formate, or methylamine as sole energy source; or heterotrophically with a variety of sugars, organic and amino acids, and alcohols (*9*). Apart from oxygen, *N*-oxides such as nitrate, nitrite, nitric oxide, or nitrous oxide can serve as electron acceptors of the respiratory process (*10*, *11*). This versatility in utilization of electron donors and acceptors is the consequence of the ability of the bacterium to redirect electron fluxes to alternative branches within its respiratory network (short-term adaptation) as well as to change the makeup of the respiratory network

(long-term adaptation) in response to environmental changes (*7*, *8*, *12–16*).

Elucidation of the composition of the network at different growth conditions and the role of each component within it have been facilitated by biochemical and physiological analyses of respiratory mutants that were created by means of targeted gene exchange techniques (*17*, *18*). As a result of these approaches, strains that have a mutation in the chromosomal gene encoding one of the redox enzymes are generated. These mutations may be either marked or unmarked, in which case the target gene is interrupted by an antibiotic resistance gene or (partly) deleted, respectively. Because the number of antibiotic resistance markers that may be used in *P. denitrificans* is limited, the advantage of the latter approach is that more than one mutation in different target genes can be created in the same strain. This technique has been extremely useful in the attempt to unravel the many respiratory branches that operate in parallel in *P. denitrificans*. At present, a number of the genes and gene clusters encoding its respiratory enzymes have been cloned (*8*), and, by using the above approach, a comprehensive set of respiratory mutants with single or multiple mutations in either of these genes, and in different combinations, has become available for detailed analyses. On the basis of these analyses, the elucidation of the organization of the network under different growth conditions has been achieved (*8*, *19*).

2. *The Makeup and Bioenergetics of the Respiratory Network*

a. Aerobic Growth. The constitutive part of the respiratory network consists of nicotinamide adenine dinucleotide (NADH) dehydrogenase, succinate dehydrogenase, ubiquinone-10, the cytochrome bc_1 complex, and cytochromes c_{550} (located in the periplasm), and c_{552} (anchored in the membrane). NADH dehydrogenase and cytochrome bc_1 are membrane-bound protein complexes by which the free energy made available by the electron transfer reactions is used for the generation of a proton gradient across the membrane. Depending on the availability of suitable carbon and energy sources as well as on terminal electron acceptors, additional components and/or branches are expressed and linked to the constitutive part of the network. When the bacterium experiences relatively high (for instance, atmospheric) oxygen concentrations it synthesizes an aa_3-type cytochrome *c* oxidase. This terminal four-subunit complex spans the membrane and catalyzes the four-electron reduction of dioxygen to water with the concomitant generation of an electrochemical potential across the membrane. The resulting electron transfer chain thus comprises three

sites of energy conservation (NADH dehydrogenase, the cytochrome bc_1 complex, and the aa_3-type oxidase), by which means the bacterium is able to generate ATP per electron very efficiently. With respect to the organization and function, the aerobic respiratory network resembles the one that is operating in mitochondria (*20*, *21*), organelles of eukaryotic cells that are optimized for energy production (Fig. 1). In *P. denitrificans*, the concentration of the aa_3-type cytochrome *c* oxidase decreases with decreasing oxygen concentrations, and the protein is virtually absent during anaerobiosis (*22*, *23*). In addition, the expression of this oxidase is twofold increased in cells grown on methanol or methylamine as compared with heterotrophically grown cells (*24–26*). Oxidases of this type are found in a wide variety of cells. Apart from their presence in eukaryotic cells, aa_3-type cytochrome *c* oxidases have been encountered in many eubacterial (both gram negative and positive), and archaebacterial (*Sulfolobus acidocaldarius*) species (*27*, *28*).

In addition to the aa_3-type oxidase, *P. denitrificans* has the genetic potential to express two other types of terminal oxidases: the bb_3-type quinol oxidase and the cbb_3-type cytochrome *c* oxidase (*7*, *12*). The three types of oxidases share common biochemical properties and architectural features (*7*, *29*). The most pronounced homology is found between the respective subunits I of the enzymes, which harbor the metal centers involved in electron transport and catalysis of oxygen

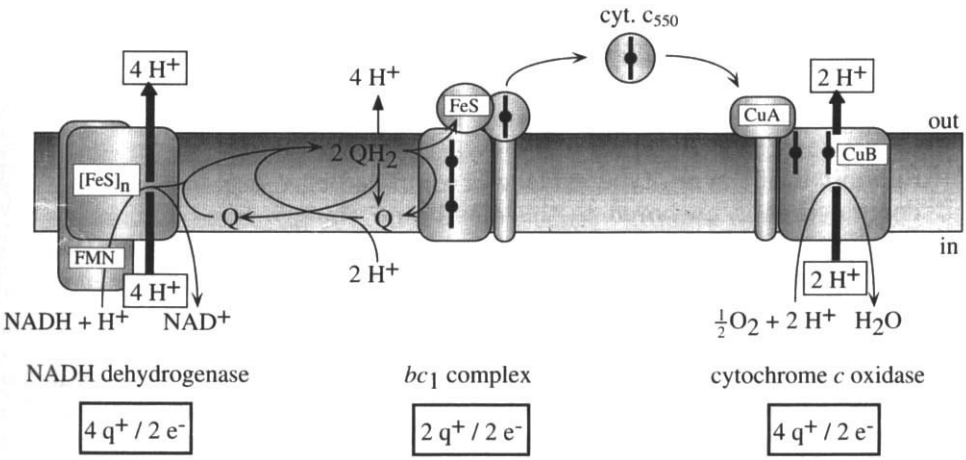

FIG. 1. Scheme of the mitochondrial respiratory chain: NADH dehydrogenase, ubiquinone (Q), the bc_1 complex, cytochrome c_{550}, and the aa_3-type cytochrome *c* oxidase. Not included is succinate dehydrogenase. Pumped protons (H^+) are boxed, scalar protons are not. Charge separation ($q/2e^-$) sites are indicated.

reduction. The subunits I all have 12 transmembrane α-helices with a total of six invariant histidine residues located in helices 2, 6, 7, and 10. These histidines are the ligands for the low- and high-spin hemes (*a* and a_3 in the aa_3-type oxidase, and *b* and b_3 in the bb_3- and cbb_3-type oxidases, respectively), and a copper ion, Cu_B, the latter two of which form the binuclear reaction center (*30*, *31*). On the basis of this resemblance, it has been postulated that the three different types of oxidases are all members of a superfamily of heme–copper oxidases sharing a common ancestor (*7*, *29*). Amino acid residues implied in the pathway of pumped protons and chemical protons are conserved in aa_3-type cytochrome *c* and bb_3-type quinol oxidases (*31*, *32*). Evidence for the suggested pathways has recently been obtained from studies on the three-dimensional structure of the aa_3-type oxidase, which was determined from X-ray analysis of the crystallized protein complex (*33*, *34*). These pathways are apparently not present in cbb_3-type oxidases, because they lack the conserved amino acid sequences at the corresponding positions of the sequence (*7*, *35*). Nevertheless, all three types of oxidases have proton pumping capacities and contribute to the generation of the electrochemical gradient (*35*). From the viewpoint that such a fundamentally important feature should be conserved among all members of the oxidase family, it may thus be that the mechanism of proton efflux is not yet understood properly. Alternatively, the proton channel in the cbb_3-type oxidases may be composed of residues different from those of the other types.

The most striking difference between these types of oxidase consists in the nature of the other subunits, which are involved in binding their dedicated electron donors and in enhancing the stability of the enzyme complex. Here, we will only focus on the electron entry sites. Subunit II of the aa_3-type oxidase is composed of a large periplasmic domain that is anchored to the membrane via two transmembrane α-helices (*33*). The soluble domain contains a binuclear Cu_A center that mediates the electron transfer between cytochrome *c* and heme *a* (*33*, *36*, *37*). With respect to its primary amino acid sequence as well as its geometry, its counterpart in the bb_3-type quinol oxidase is very similar (*28*, *38*). The most pronounced difference is the lack of a Cu_A center, which makes it unsuited to react with cytochromes *c*. Instead, it receives electrons directly from quinol. The electron entry pathway in the cbb_3-type oxidase is poorly understood. Apart from subunit I (CcoN), the oxidase consists of two membrane-anchored subunits, one of which has a single heme *c* (CcoO), whereas the other one has two hemes *c* (CcoP) (*35*, *39*, *40*). Mutant studies have revealed that cyto-

chrome bc_1, or cytochrome c_{550}, but not cytochrome c_{552}, can act as electron donor for this oxidase (*8*). Perhaps the two hemes in CcoP make up an electron transfer pathway between the cytochrome bc_1 complex and the oxidase, whereas CcoO is responsible for electron transfer between the soluble cytochrome and the oxidase.

It is not only on the basis of electron entry sites that these types of oxidases are different. As compared with the aa_3- and bb_3-type cytochrome *c* oxidases, the cbb_3-type oxidase has a ~10-fold higher affinity for oxygen (*41*). Not surprisingly, therefore, expression of the latter oxidase increases at decreasing oxygen concentrations (*6*, *42*). Oxidases of the cbb_3-type or their allocated gene clusters have thus far been characterized in *P. denitrificans* (*35*), *Rhodobacter capsulatus, Azotobacter vinelandii, Agrobacterium tumefaciens, Pseudomonas aeruginosa* (*40*), and *Rhodobacter sphaeroides* (*27*), and in several members of the Rhizobiaceae (*39*, *42*, *43*). The latter organisms are able to fix atmospheric nitrogen in symbiosis with a legume host plant, during which interaction the bacteria are lodged in the plant nodules. The oxygen concentration in these specific plant compartments is extremely low to prevent irreversible oxidation of nitrogenase, the enzyme responsible for nitrogen fixation. In order to keep the electron fluxes through the respiratory network going the bacteria rely almost exclusively on the high-affinity cbb_3-type oxidase.

The bb_3-type quinol oxidase of *P. denitrificans* is the counterpart of the well-known *Escherichia coli* bo_3-type quinol oxidase (*12*, *44*). This type of oxidase is common in all genera of eubacteria (*28*). Because these redox enzymes couple the oxidation of quinol directly to the reduction of oxygen, this electron transfer route is less efficient with respect to free energy transduction than those involving the energy-generating cytochrome bc_1 complex. Little is known as to whether and how the expression of the quinol oxidase is fine-tuned in response to environmental changes. A model for electron transfer during heterotrophic growth is shown in Fig. 2A.

b. Anaerobic Growth. In the absence of molecular oxygen, electron flow is dependent on the availability of *N*-oxides that may serve as alternative electron acceptors (*8*, *10*, *44*, *45*, *46*). At the shift from oxygen limitation to anaerobiosis, the makeup of the respiratory network drastically changes. The expression of nitrate, nitrite, nitric oxide, and nitrous oxide reductases as well as of the blue copper-containing electron carrier pseudoazurin is established, and in a concerted action these terminal oxidoreductases couple the removal of electrons from the respiratory network to the reduction of the corresponding

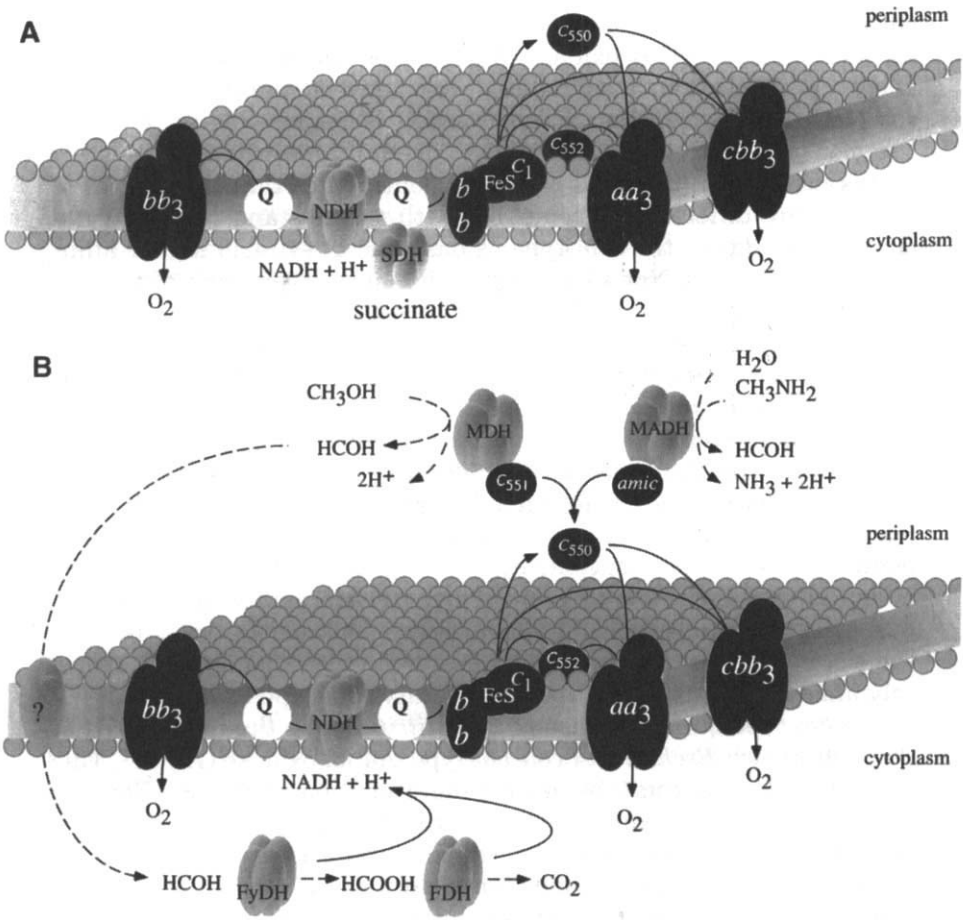

FIG. 2. The respiratory network of *P. denitrificans* during (A) aerobic heterotrophic growth and (B) methylotrophic growth. Common components of the two networks: NADH dehydrogenase (NDH), ubiquinone (Q), the cytochrome bc_1 complex (bb, FeS, c_1), cytochromes c_{550} and c_{552}, and the three oxidases: the aa_3-type cytochrome c oxidase (aa_3), the cbb_3-type cytochrome c oxidase (cbb_3), and the bb_3-type quinol oxidase (bb_3). Succinate dehydrogenase (SDH) is relevant during aerobic heterotrophic growth. Methanol dehydrogenase (MDH), methylamine dehydrogenase (MADH), amicyanin (amic), cytochrome c_{551i} (c_{551}), formaldehyde dehydrogenase (FyDH), formate dehydrogenase (FDH), and a putative formaldehyde carrier (?) are induced during methylotrophic growth. Solid arrows indicate the pathways of electron transfer; dashed arrows indicate molecule conversion and transfer.

N-oxides, ultimately yielding molecular nitrogen (denitrification). With respect to free energy transduction, these pathways are less efficient as compared to aerobic respiration because either they bypass the cytochrome bc_1 complex (route to nitrate reductase), or the branches terminate in non-energy-conserving enzymes (routes to the nitrite, nitric oxide, and nitrous oxide reductases). In addition, growth under this condition brings the bacterium in the apparent paradox of maintaining high electron fluxes to support competitive growth on the one hand, and of preventing the accumulation of the toxic intermediates nitrite and nitric oxide on the other hand. It may be anticipated that global and local regulatory pathways controlling the expression and/or activity of these oxidoreductases are optimally integrated to solve this paradox. Indeed, it has been determined that a number of regulatory proteins, among which are two members of the fumarate nitrate reductase (FNR) family of transcription activators (*8*, *47*), are involved in regulation of gene expression during the aerobic–anaerobic shift.

c. Autotrophic Growth. In the situation that *P. denitrificans* experiences a shortage of heterotrophic substrates, it can switch to autotrophic growth, during which hydrogen or thiosulfate are oxidized by hydrogenase or a thiosulfate-oxidizing enzyme, respectively (*48–50*). Carbon supply is accomplished by the fixation of atmospheric carbon dioxide via the Calvin cycle under this growth condition. The bacterium is also able to grow on C_1 substrates such as methanol or methylamine (*19*), a process considered as autotrophic growth too, because these carbon sources are oxidized merely with the purpose to gain energy (*26*).

In the presence of methanol as the sole source of energy, *P. denitrificans* induces the expression of the *mxa* gene cluster encoding methanol dehydrogenase (MDH) and its dedicated electron acceptor cytochrome c_{551i} (*14*, *51*). Both proteins are located in the periplasm and in subsequent redox steps they connect the oxidation of methanol to the reduction of cytochromes c_{550} and c_{552}. MDH consists of a large subunit (66 kDa; α-MDH) and a small subunit (9 kDa; β-MDH) that are complexed together in an α_2–β_2 tetrameric configuration (*52*, *53*). The large subunit has eight topologically identical antiparallel β-sheets arranged in a superbarrel structure with radial symmetry. The center of this structure makes up the active site pocket where the cofactor of the enzyme, pyrroloquinoline quinone (PQQ), is noncovalently incorporated in the protein structure, and in close contact with a Ca^{2+} ion. Methanol-oxidizing branches are found in a wide variety of methylotrophic bacteria (*54*). Apart from *P. denitrificans*, much of

the current knowledge on the physiology and molecular genetics of this system has been obtained from studies on the facultative methylotrophic bacteria *Methylobacterium extorquens* AM1, *Methylo bacterium organophilum* XX, and *Methylobacterium organophilum* DSM 760 (reviewed in Ref. *55*). Like in *P. denitrificans*, the methanol-oxidizing branch of these bacteria is composed of MDH, a dedicated cytochrome *c*L, a cytochrome *c*H (L and H refer to low and high isoelectric points, respectively), and a cytochrome *c* oxidase. The work of Lidstrom *et al.* (*55*) further revealed that the synthesis of a fully active methanol-oxidizing branch requires a total of at least 32 genes, among which are the *pqq* genes involved in cofactor biosynthesis, and a comprehensive set of so-called *mxa, mxb, mxc,* and *mxd* genes, some of which encode the structural enzymes, others of which encode enzymes involved in calcium insertion, and proteins involved in regulation of gene expression and protein activity (*55*).

Growth on methylamine is accompanied by the appearance in the periplasm of methylamine dehydrogenase and its electron acceptor amicyanin, both of which are encoded by the *mau* gene cluster (*15, 56–58*). Like MDH, MADH has an α_2–β_2 configuration made up by a small (16 kDa; β-MADH) and a large (47 kDa; α-MADH) subunit, which is also shaped like a superbarrel with radial symmetry (*59, 60*). The active site, however, is found in the small subunit (*61*). This site is created after the cross-linking and modification of two tryptophan residues of the peptide chain, resulting in the formation of the prosthetic group tryptophan-tryptophyl quinone. Electrons derived from the oxidation of methylamine are transferred via the blue copper protein amicyanin to the electron transport network at the level of cytochrome *c* (cyt c_{550}) (*62, 63*). Methylamine-oxidizing branches similar to that of *P. denitrificans* have also been identified in *P. versutus*, and *M. extorquens* AM1. Obligate (*Methylobacillus flagellatum* KT) and restricted facultative (*Methylophilus methylotrophus* W3A1) methylotrophic bacteria use similar branches for the oxidation of methylamine, but the dedicated electron acceptor of MADH in these bacteria appears to be either another type of blue copper protein, azurin (*64*), or a cytochrome *c* (*65, 66*), respectively, rather than amicyanin. The presence or absence of the latter redox carrier correlates with the presence or absence of its allocated gene, *mauC*, in the *mau* gene clusters of the different species.

In addition to the proteins expressed specifically during and involved in the oxidation of methanol and methylamine, a cytochrome c_{553i} is expressed during growth on these C_1 substrates (*5, 67*). The gene encoding this cytochrome (*cycB*) has been cloned and shown to

be part of the *xox* gene cluster (*68*). Surprisingly, the products of the genes located upstream and downstream of *cycB* (*xoxF* and *xoxJ*, respectively) have a large degree of similarity with α-MDH and MxaJ, respectively. The role of this putative oxidizing branch still remains obscure, because mutational analysis of this gene cluster did not reveal a clear function of the proteins (*68*).

The oxidation product of both methanol and methylamine is formaldehyde, which crosses the membrane into the cytoplasm. This transport process has been suggested to involve a specific formaldehyde carrier (*69*). In the cytoplasm, formaldehyde is further oxidized to formate via two consecutive reactions. In the first reaction, an NAD-linked glutathione-dependent formaldehyde dehydrogenase (FlhA) catalyzes the oxidation of formaldehyde into *S*-formylglutathione (*70*). In the second reaction, the latter molecule is converted into formate by *S*-formylglutathione hydrolase, which is a human esterase D homologue (*71*). The *flhA* gene cluster of *P. denitrificans* encoding the two enzymes has recently been identified upstream of the *xox* gene cluster (*72*). Finally, formate is oxidized to carbon dioxide predominantly by an NAD-dependent formate dehydrogenase (*54*). It has been reported, however, that *P. denitrificans* can synthesize isoenzymes of the formaldehyde and formate dehydrogenases that are NAD independent (*73*). A schematic view of the respiratory network that operates during C_1 metabolism is presented in Fig. 2B.

The free energy yield from the six-electron oxidation of methanol or methylamine to carbon dioxide may vary from 12 to 24 charge separations (q) per mole of substrate, depending on the types of oxidases and dehydrogenases that contribute to the electron transfer reactions. Two of the electrons that are released during the first step of oxidation of these sources are transferred to either of the two cytochrome *c* oxidases, via cytochrome *c* or amicyanin, yielding 4 q/mol substrate. In the case that the formaldehyde and formate dehydrogenases are both NAD dependent, transfer of the remaining four electrons may yield an additional 16 to 20 q/mol substrate, depending on the partitioning of electrons among the quinol oxidase on the one hand and the cytochrome bc_1 complex and the cytochrome *c* oxidases, on the other hand, at the level of the *Q* pool. In case the NAD-independent formaldehyde or formate dehydrogenases also contribute to the catabolic reactions, these values drop to 8 to 12 q/mol substrate because the energy-conserving NADH dehydrogenase complex is bypassed.

Counterparts of many redox enzymes of *P. denitrificans* are also present in *P. versutus*. Moreover, the DNA sequences of the genes and gene clusters encoding cytochrome c_{550} (*cycA*), the aa_3-type oxidase (*cta*

gene clusters), and the methylamine-oxidizing branch (*mau* gene cluster) have been shown to be strongly similar to their counterparts in *P. denitrificans* (*73a*). These findings indicate that the organization and function of the respiratory networks in both organisms resemble each other to a great extent. This resemblance is in agreement with the physiology of *P. versutus*, which has strong similarities to that of *P. denitrificans*. One of the differences appears to be that the former organism is unable to use methanol as source of energy.

B. Respiratory Genes and Their Expression

1. Control of Expression of Respiratory Genes

The expression of the components of the methanol- and methylamine-oxidizing branches is subject to complex regulatory cascades that have to orchestrate the optimal composition of the respiratory network under these growth conditions in order to maintain respiratory electron flows at competitive rates, on the one hand, yet to prevent the accumulation of the toxic intermediate formaldehyde on the other. Moreover, parts of these signal transduction systems coordinate gene expression according to an energetic hierarchy, ensuring that the C_1-oxidizing branches are expressed only when the cell is unable to metabolize energetically more favorable substrates (*19*). This view is corroborated by extensive physiological and biochemical studies on this type of metabolism. MADH and amicyanin are synthesized only when the cell uses methylamine (and to a lesser extent other alkylamines) as sole source of energy (*15*, *74*). MDH and XDH and their dedicated cytochromes, on the other hand, are expressed not only during growth on methanol but also during growth on methylamine or choline. Because the oxidation of all these carbon sources yields formaldehyde, it has been postulated that the latter molecule is an important trigger in the regulation of expression of their allocated gene clusters (*73*). The synthesis of all enzymes involved in the oxidation of methanol or methylamine is blocked when heterotrophic growth substrates are available next to these C_1 substrates (*14*, *15*). Growth during C_1 metabolism also affects the regulation of expression of the other components of the branches, cytochrome c_{550} and the cytochrome *c* oxidases. The amount of these components increases two- to fivefold as compared to heterotrophic growth (*24*). Apparently, this increased supply meets the demands on increased velocities of electron transfer within this part of the respiratory network. A number of different regulatory proteins that control

the expression of the *flh, xox, mxa*, and *mau* gene clusters (*75*), as well as that of the *cco* and *qox* gene clusters, have been identified (*8*).

a. mxa Gene Cluster. Expression of the *mxa* genes is controlled by the gene products of the *mxaXYZ* genes, which are located upstream of the structural *mxa* gene cluster (*14*). MxaY and MxaX are a protein histidine kinase and a DNA-binding response regulator, respectively, a set of proteins that belongs to the family of two-component regulators. As suggested above, the effector molecule for the sensor domain of MxaY is probably formaldehyde. The general principle for signal transduction via two-component regulatory systems is that binding of the effector molecule triggers the autophosphorylation of the kinase, after which the phosphate group is transferred to the response regulator. Once phosphorylated, the latter may bind to the promoter region of its target gene in order to facilitate transcription by the RNA polymerase (*76*). Surprisingly, however, MxaY was shown to be dispensable in this cascade, suggesting that an alternative kinase takes over its role (*77*). The role of MxaZ in this cascade is still unclear. The MxaYX regulatory system appears to be specifically dedicated to the regulation of expression of the *mxa* genes; *mxaX* mutants showed an unimpaired expression of the *mau*, *flhA*, and *xox* genes (*14*, *75*). A two-component system, MxcQE, with a function similar to that of MxaYX, has now also been identified in *M. organophilum* XX. Its allocated gene cluster, however, is separated more than 40 kb from its target *mxa* gene cluster (*78*).

b. mau Gene Cluster. The *mau* gene cluster of *P. denitrificans* consists of 11 genes. Of these, 10 encode the structural proteins and proteins involved in cofactor biosynthesis and are transcribed in one direction; the 11th one is located upstream and is divergently transcribed (*15*, *57*, *58*). It encodes MauR, which is a transcription activator that belongs to the family of one-component LysR-type regulators. The spatial organization of the functional domains involved in DNA binding, signal perception, and dimerization in the members of this family is conserved (*79*). Usually the target locus of this type of regulator codes for a set of proteins that oxidize a particular substrate. The substrate molecule in turn serves as the trigger for the activation of the LysR regulator. This characteristic would be in agreement with the suggestion that methylamine is the molecule that triggers the expression of the *mau* gene cluster. The current view with respect to the mode of action of LysR-type regulators is that signal perception (i.e., binding of the activator molecule) induces dimerization of the regulator followed by binding to a target site up-

stream of the promoter. As a result, the dimer may come into contact with RNA polymerase, after which transcription is initiated. In agreement with this view is the observation that MauR binds to the *mau* promoter region in a band-shift assay (*80a*). The target site for LysR-type activators is usually a conserved T-N11-A motif that harbors small palindromic sequences at its ends. Such a motif, however, has not been recognized in the *mau* promoter region, indicating that the target site of MauR is slightly different from the conserved one. The target site for CatR, another member of the family of the LysR-type activators, is G-N11-A (*80b*), suggesting that small deviations of the target sequence indeed occur. Promoter probe studies have further shown that *mau* gene expression increases almost 1600-fold during growth on methylamine as compared to heterotrophic growth. This increase was not observed in the MauR mutant, which confirms that MauR is responsible for the increase in gene expression in the wild type (*80a*). The expression of the *mauR* gene is more or less constant, and independent of the growth condition or the concentration of MauR. Apparently, its expression is not autoregulated, a feature different from that of most other *lysR*-type genes. A counterpart of *mauR* has also been described in *P. versutus,* although the orientation of it is opposite to that of the *P. denitrificans* gene (*81*). Analysis of the corresponding region upstream of the *mau* gene cluster from *M. extorquens* AM1 did not reveal sequences with similarity to *mauR* (*56*).

c. Hierarchical Control. Apart from regulation by their cognate activators, the regulation of the expression of both *mxa* and *mau* gene clusters is subject to some kind of hierarchical control that suppresses transcription during heterotrophic growth. Indeed, it has been shown that the expression of the *mau* genes is virtually blocked in the situation that the bacterium grows in the simultaneous presence of succinate and methylamine. Further, both MADH and MDH are absent once succinate is added to the growth medium in addition to their corresponding substrates (*19*). The view that a global transcription activator is responsible for these phenomena has recently been corroborated by the analysis of a mutant disturbed in many aspects of C_1 metabolism (*75*). This mutant was unable to grow on methanol, methylamine, or choline. Moreover, the expression of the *flhA, mxa, mau,* and *xox* genes was completely blocked. These pleiotropic effects were explained by assuming that the mutated gene in this strain encodes a regulator that affects the expression of all these C_1 genes and gene clusters. Apparently, this regulator is not a repressor protein

because in the mutant in which the regulator gene has been knocked out one would expect constitutive expression rather than repression. Therefore, it has been suggested that this protein acts as a second activator in synergism with either of the two dedicated activators of *mxa* and *mau* gene expression. If this view is correct, one may expect that the presence and/or activity of this second activator is suppressed during heterotrophic growth. The identification of its allocated gene has been facilitated by the isolation of a genomic locus that fully complements the mutation. A scheme of the regulatory pathways that control gene expression during C_1 metabolism is shown in Fig. 3.

d. Redox Control. The expression of *cycA* and the *cta* and *cco* gene clusters, encoding cytochrome c_{550} and the aa_3-type and cbb_3-type cytochrome *c* oxidases, respectively, is also controlled by regulatory pathways that respond to the switch from heterotrophic growth to C_1 me-

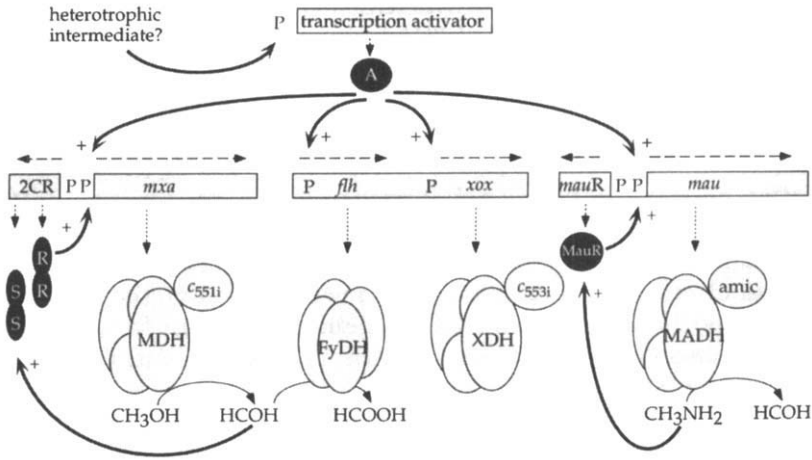

FIG. 3. Model of regulatory pathways involved in C_1 metabolism in *P. denitrificans*. Genes and gene clusters are boxed; promoter regions (P) are designated. Structural proteins are methanol dehydrogenase (MDH), methylamine dehydrogenase (MADH), formaldehyde dehydrogenase (FyDH), the product of the *xox* genes (XDH), the cytochromes c_{551i} (c_{551i}) and c_{553i} (c_{553i}), and amicyanin (amic). Regulatory proteins (shaded) are the proposed formaldehyde sensor MxaY (S, dimer), and its allocated regulator MxaX (R, dimer) encoded by their corresponding *mxa* two-component regulatory genes (2CR), the LysR-type activator of *mau* gene expression (MauR), and the proposed global activator (A). Dotted arrows represent the transcription–translation process. Dashed arrows indicate the direction of transcription. Thin solid lines indicate substrate conversion. Thick solid lines indicate the processes involved in signal transduction and regulation (+, positive; −, negative).

tabolism. The cbb_3-type oxidase is hardly detectable in cells grown heterotrophically at relatively high (atmospheric) oxygen concentrations, but its synthesis increases when the cell experiences a shortage of oxygen or when it grows on C_1 compounds (*6*, *22*). In the former situation the electron output rate is limiting, whereas in the latter one the electron input rate increases, thus one might expect that the components in the respiratory network become more reduced under these growth conditions. The suggestion that a change of the redox potential of one of these components is the trigger for increased expression of the *cco* gene cluster has recently been corroborated by the finding of a homologue of the *E. coli* FNR protein in *P. denitrificans*, designated FnrP (*35*). FNR in *E. coli* dictates the extent of expression of a number of genes involved in the aerobic–anaerobic switch (*82*, *83*). The protein has a redox-sensitive [4Fe–4S] cluster that is supposed to either sense the oxygen concentration or the redox state of one of the components of the respiratory network. Reduction of the cluster triggers a conformational change, on which the protein dimerizes and binds to its target site, a so-called FNR-box (*82*, *84*). This box harbors a conserved TTGAT–ATCAA sequence motif, which is usually located directly upstream of the RNA polymerase binding site. This organization makes sure that the FNR dimer and RNA polymerase bind next to each other on the DNA, thereby allowing physical contact between these two protein complexes. Once this occurs transcription starts. The functional domains of FNR are also present in FnrP from *P. denitrificans* (*47*). A knock-out of its allocated gene resulted in a number of effects on gene expression, among which was a decrease of *cco* gene expression to a residual 25% of the wild-type level, and a threefold increase of *qox* gene expression. In agreement with this observation was the finding of an FNR-box within the promoter regions of the *cco* and *qox* gene clusters. The mutation did not affect the expression of cytochrome c_{550} or the aa_3-type oxidase. Moreover, the promoter regions of their allocated genes do not contain an FNR-box. Analyses of strains with promoter–reporter gene fusions have revealed that the expression of the *cycA* gene increases 10- to 20-fold in cells grown on methanol or methylamine as compared to succinate-grown cells (*85*). Further, the authors came across two different *cycA* promoters. Perhaps one of these promoters is switched on for elevated gene expression during C_1 metabolism. The amount of aa_3-type oxidase increases twofold during C_1 metabolism. As yet, virtually nothing is known about the nature and mode of action of the transcription regulators controlling their expression in response to

the growth condition. Whether one of the regulatory proteins identified in the C_1 signal transduction network is required for the observed boost in induction of gene expression during growth on C_1 substrates is a matter of speculation.

III. Structure and Function of the MADH Redox Chain Components

A. Structure and Function of Amicyanin and Cytochrome c_{550}

1. *Amicyanin*

a. Structure. Amicyanin (AmCu) is a member of the type 1 blue (cupredoxin) family of copper proteins. The protein functions as the obligate electron acceptor for the enzyme methylamine dehydrogenase in the methylamine-utilizing redox chain of *P. versutus* and *P. denitrificans* (*86*). The primary structures of amicyanin from these two sources (*86*, *87*) are compared in Table I. It is clear that the homology between the two amicyanins is high, with 63% identity of amino acid residues. The three-dimensional structure of the oxidized AmCu(II) form of the protein from *P. versutus* has been solved by X-ray crystallography (*88*), and the NMR-derived solution structure of the diamagnetic reduced protein is also available (*89*). Amicyanin from *P. denitrificans* has also been studied crystallographically in its Cu(II) state (*90*, *91*) with the structure obtained showing very high similarity to that of the *P. versutus* protein (*vide infra*). By far the most interesting aspect of the crystallographic studies on *P. denitrificans* amicyanin is the availability of the structure of its binary complex with MADH (*92*) and also that of a ternary complex with MADH and cytochrome c_{551i} (*93*, *94*). These studies will be discussed in more detail in a later section of this review.

The structural studies on amicyanin from *P. versutus* show that the protein consists of nine β-strands that form into two antiparallel β-sheets, giving the molecule an overall structural motif known as a β-sandwich (see Fig. 4). This overall topology is very similar to that of other structurally characterized cupredoxins, with the homology to plastocyanin being greatest (*87*). The only notable difference between amicyanin and most other cupredoxin structures is the presence of a 21-residue N-tereminal extension that forms an extra β-strand in the structure. The recently published structural studies (*95*, *96*) on the type 1 blue copper protein rusticyanin show that it, too, possesses an

TABLE I

COMPLETE AMINO ACID SEQUENCES OF AMICYANINS FROM *Paracoccus versutus* AND *Parococcus denitrificans*[a]

P. versutus	Gln	Asp	Lys	Ile	Thr	Val	Thr	Ser	Glu	Lys	Pro	Val	Ala	Ala	Ala	15
P. denitrificans		Asp	Lys	Ala	Thr	Ile	Pro	Ser	Glu	Ser	Pro	Phe	Ala	Ala	Ala	
P. versutus	Asp	Val	Pro	Ala	Asp	Ala	Val	Val	Val	Gly	Ile	Glu	Lys	Met	Lys	30
P. denitrificans	Glu	Val	Ala	Asp	Gly	Ala	Ile	Val	Val	Asp	Ile	Ala	Lys	Met	Lys	
P. versutus	Tyr	Leu	Thr	Pro	Glu	Val	Thr	Ile	Lys	Ala	Gly	Glu	Thr	Val	Tyr	45
P. denitrificans	Tyr	Glu	Thr	Pro	Glu	Leu	His	Val	Lys	Val	Gly	Asp	Thr	Val	Tyr	
P. versutus	Trp	Val	Asn	Gly	Glu	Val	Met	Pro	His	Asn	Val	Ala	Phe	Lys	Lys	60
P. denitrificans	Trp	Ile	Asn	Arg	Glu	Ala	Met	Pro	His	Asn	Val	His	Phe	Val	Ala	

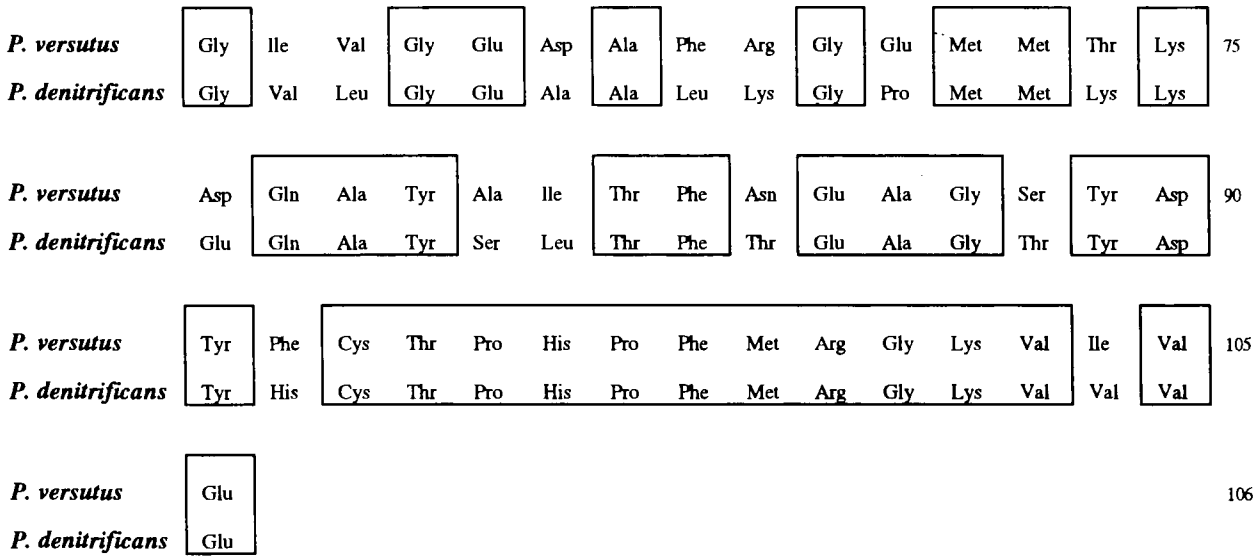

[a] Data for *P. versutus* from Ref. *73a*; data for *P. denitrificans* from Ref. *63*. Identical residues are boxed.

FIG. 4. Representation of the three-dimensional structure of *P. versutus* amicyanin.

N-terminal extension, but in this case it is 35 residues long and is involved in three β-strands that contribute to both β-sheets of the protein.

The single copper atom that makes up the active site of amicyanin is found at one end of the β-sandwich (Fig. 4). The metal is strongly coordinated by the S of a cysteine (Cys-93) and the N^{δ} atoms of two histidine ligands (His-54 and His-96). The copper atom is displaced by 0.4 Å from the plane of these three equatorial ligands in the direction of a distant axial methionine ligand. The active site of oxidized amicyanin from *P. versutus* is shown in Fig. 5 and the bond lengths and angles found for this protein and that from *P. denitrificans* are listed in Table II. From the numbering of the amino acids in Fig. 5 it is clear that one of the histidine ligands (His-54, *P. versutus* numbering) is found at some distance in the primary structure from the three other coordinating residues, which are found close together on a single loop. The C-terminal ligand-containing loop is a common feature of all the cupredoxins and the length of this loop in amicyanin is the shortest of all the type 1 blue copper proteins.

Another feature of amicyanin that is common to all structurally investigated cupredoxins is the presence of a hydrophobic patch on the protein surface, which surrounds the exposed imidazole ring of

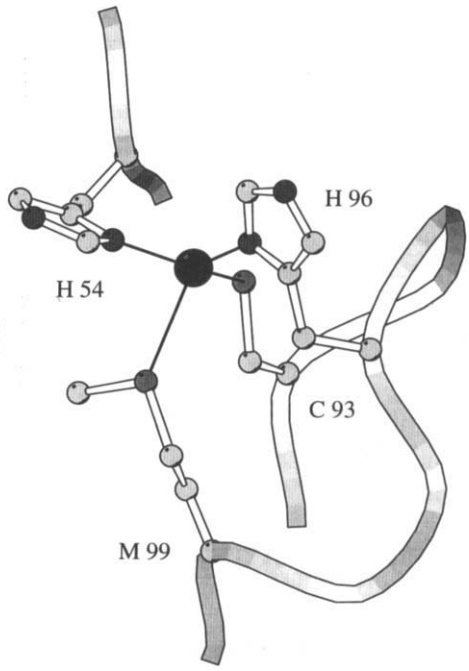

FIG. 5. Representation of the Cu site of *P. versutus* amicyanin, highlighting the loop that contains the three copper ligands Cys-93, His-96, and Met-99. The copper atom is indicated by the dark sphere in the center of the figure.

the C-terminal histidine ligand (His-96 in the case of amicyanin). This patch has been proposed as the main port of entry and exit of electrons into and out of the active sites of cupredoxins.

b. Spectroscopy. Spectroscopically, oxidized amicyanin from *P. versutus* is typical of a type 1 blue copper protein, with a main visible absorption band at 596 nm, due to a $p\pi S(Cys) \rightarrow d_{x^2-y^2}$ Cu(II) charge transfer transition (*97–99*) and a hyperfine coupling constant of 5.3 mT in its EPR spectrum. It is known that although the cupredoxins are classified together on the basis of spectroscopic similarities, the fine details of these features differ from one member of the family to another. Two distinct classes of cupredoxins have been identified on the basis of specific spectroscopic features. These are the type 1 axial sites in which the g_x and g_y values are close together and which have little absorption at around 460 nm in their visible spectra [this second electronic transition has been assigned as a $\sigma S(Cys) \rightarrow d_{x^2-y^2}$ Cu(II)

TABLE II

BOND DISTANCES AND ANGLES AT THE ACTIVE SITE OF AMICYANIN FROM *P. versutus* AND *P. denitrificans*

Parameter	AmCu(II) *P. versutus*	AmCu(II) *P. denitrificans*
Resolution (Å)	2.15	1.31
Bond lengths (Å)		
Cu–$N^{\delta 1}$ (His-54)[a]	2.04	1.95
Cu–S^{γ} (Cys-93)	2.13	2.11
Cu–$N^{\delta 1}$ (His-96)	2.13	2.03
Cu–S^{δ} (Met-99)	2.84	2.90
Bond angles at copper atom (degrees)		
$N^{\delta 1}$ (His-54)–Cu–S^{γ} (Cys-93)	132	136
$N^{\delta 1}$ (His-54)–Cu–$N^{\delta 1}$ (His-96)	104	104
$N^{\delta 1}$ (His-54)–Cu–S^{δ} (Met-99)	84	84
S^{γ} (Cys-93)–Cu–$N^{\delta 1}$ (His-96)	111	112
S^{γ} (Cys-93)–Cu–S^{δ} (Met-99)	117	110
$N^{\delta 1}$ (His-96)–Cu–S^{δ} (Met-99)	101	100

[a] *Paracoccus versutus* numbering.

charge transfer transition (*98*, *99*)]. The second class of cupredoxin active sites has more rhombic EPR spectra features accompanied by an increased absorption at 460 nm (*97–99*). The amicyanins from *P. versutus* (*100*) and *P. denitrificans* (*62*, *101*) both have type 1 axial sites, which is thought to be consistent with a relatively long Cu–S (Met) axial bond length [crystallographic studies have shown that in type 1 rhombic sites the Cu–S(Met) bond is significantly shorter (*95*, *96*, *102–105*)]. The relationship between the spectroscopy and active site structure of these two classes of type 1 copper center is supported by resonance Raman studies (*106*, *107*) showing that the more rhombic sites have a longer Cu–S(Cys) bond length.

Recently an additional spectroscopic technique has been utilized to quantify the extent of the axial interaction at the active sites of cupredoxins. This involves the observation and interpretation of the paramagnetically shifted signals in the ^1H NMR spectrum of the oxidized protein, and the pioneering work has been carried out on amicyanin (*108*). It has been possible for the first time to observe shifted ligand proton (resonances and assign them using exchange spectroscopy on 50:50 mixtures of oxidized and reduced samples, so as to correlate the paramagnetic resonances with their assigned diamagnetic counterparts. The paramagnetic ^1H NMR spectra of wild-type amicyanin, two amicyanin mutants (*vide infra*), and type 1 blue cop-

per protein azurin are shown in Fig. 6. On comparing the spectra for amicyanin and azurin it is clear that in the latter the $C^{\gamma}H$ resonances of the axial Met ligand are not shifted outside of the diamagnetic envelope, whereas in amicyanin they are found at ~11–12 ppm. Because the observed shifts are mainly due to Fermi-contact contributions (i.e., delocalization via covalent bonds) this demonstrates the presence of covalency of the Cu–S(Met) interaction in amicyanin and not in azurin. This is also consistent with the shorter reported Cu–S (Met) distance in amicyanin (2.8 Å) as compared to azurin (3.1 Å). One of the amicyanin mutants has a rhombic type 1 site (*vide infra*) and consistent with this the shift of the $C^{\gamma}H$ Met resonances is much larger (see Fig. 6C).

c. pH Switch. A distinctive feature of amicyanin is that, in the reduced form, the ligand His-96 protonates with a pK_a of 6.7. This behavior was originally observed in NMR studies (*109*, *110*) and later in extended X-ray absorption fine structure (EXAFS) (*111*), kinetic (*112*), and electrochemical (*113*) experiments. The protonation of His-96 results in a trigonal geometry at the Cu(I) center. Because such a coordination environment is favorable for Cu(I), as compared to the cupric form of the protein, an increase in the reduction potential, on protonation, is observed (Fig. 7). This behavior of amicyanin is another feature that strengthens the analogy to plastocyanin (PCu), which also undergoes a similar active site protonation (*114–118*). In the case of PCu(I), crystallographic studies have been carried out at various pH values (*117*). In these investigations structural details of the protonation processes are obtained and these are illustrated qualitatively in Fig. 8. The presence of a second conformation of the protonated histidine, as depicted in Fig. 8, is evident in NMR studies on both amicyanin (*110*) and plastocyanin (*118*). An intriguing difference between PCu(I) and AmCu(I) lies in the pK_a value for the protonatable histidine ligand. In PCu(I), a value of ~5 is found whereas the pK_a in AmCu(I) is almost 2 pH units higher. The possible physiological role that the active site protonation plays in the case of amicyanin will be addressed later in this review. However, at this stage it is interesting to note that plastocyanin functions in the inner thylakoid of the chloroplast, where the pH is known, under illumination, to be quite acidic, whereas amicyanin is thought to function physiologically at more neutral pH values. The type 1 blue copper protein pseudoazurin also undergoes an active site protonation, in its reduced state, with a pK_a value similar to that of plastocyanin (*119–121*).

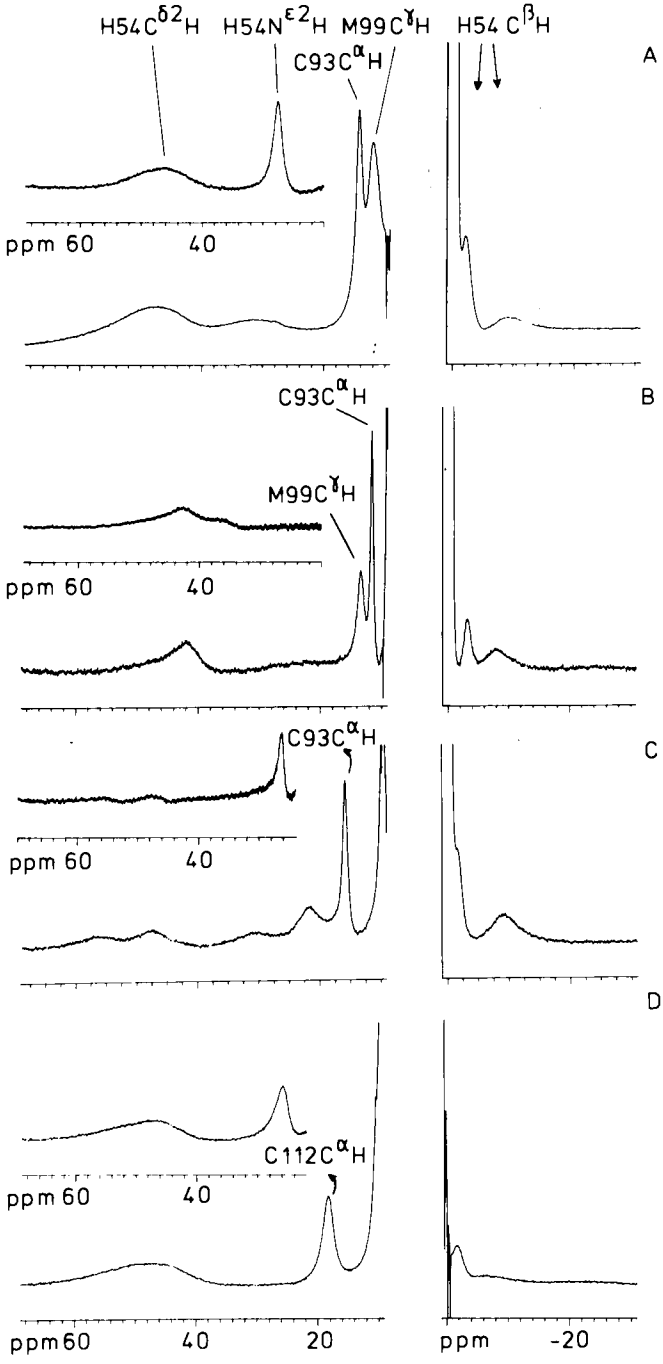
H54C$^{\delta 2}$H
H54N$^{\varepsilon 2}$H
M99C$^{\gamma}$H
H54 C$^{\beta}$H
C93C$^{\alpha}$H
A
ppm 60
40
C93C$^{\alpha}$H
B
M99C$^{\gamma}$H
ppm 60
40
C93C$^{\alpha}$H
C
ppm 60
40
D
C112C$^{\alpha}$H
ppm 60
40
ppm60
40
20
ppm
-20

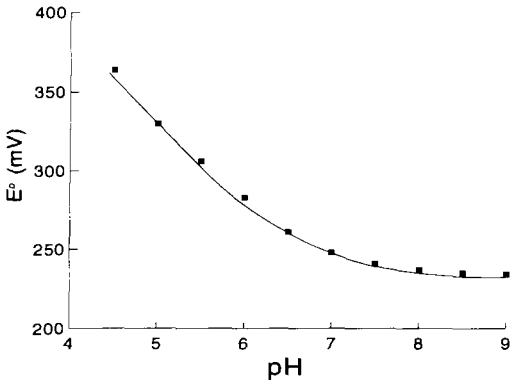

FIG. 7. Variation of the reduction potential (E°) of wild-type amicyanin with pH (I = 0.10 M, NaCl). The values are obtained from cyclic voltammetry and are all referenced to the NHE at 22°C. The line shown is the fit to the following equation (*113*): E° (pH) = E° (high pH) + (RT/nF) ln(1 + [H^+]/K_a^{red}).

d. Electron Self-Exchange. Amicyanin functions as an electron transfer protein. A basic property of all redox couples is the process of electron self-exchange, whereby the two oxidation states involved interconvert according to the following equation:

$$\text{AmCu(I)} + \text{AmCu(II)} \rightleftharpoons \text{AmCu(II)} + \text{AmCu(I)}.$$

The study of electron self-exchange rates are therefore facilitated by the fact that the process has no driving force. The self-exchange rate constant provides an intrinsic measure of the electron transfer capabilities of a redox metalloprotein. Reported self-exchange rate constants for cupredoxins range from 10^3 to 10^6 M^{-1} sec^{-1} (*122*). In all cases it is believed that type 1 blue copper proteins self-exchange via their hydrophobic patches and that electron transfer occurs through the exposed histidine ligand. However, this has only been proved in the case of the cupredoxin azurin (*123–125*). The observed self-exchange rate constant (25°C) of 1.2 × 10^5 M^{-1} sec^{-1} for amicyanin at

FIG. 6. One-dimensional water eliminated Fourier transform spectroscopy (WEFT) spectra of (A) wild-type amicyanin; (B) the amicyanin mutant H96D; (C) the amicyanin mutant H^{96}PFM → H^{96}QGAGM; (D) wild-type *Pseudomonas aeruginosa* azurin. The diamagnetic region from 9 to 1 ppm has been omitted from the centers of the spectra. The insets show the spectra in H_2O, where an additional peak from an exchangeable proton appears. Peak assignments for wild-type amicyanin are given at the top of panel A. All spectra were collected at 32°C on samples containing 50 mM phosphate, pH 7.0.

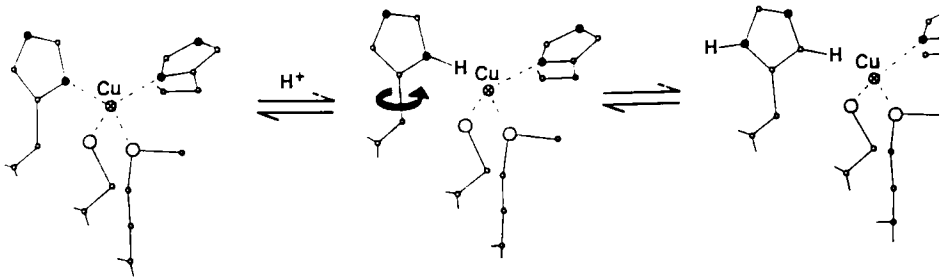

FIG. 8. The H^+-induced dissociation of the Cu(I)—N(His-96) bond of amicyanin, and the existence of two conformers of the protonated form.

pH 8.2, which is almost independent of ionic strength (*110*), is intermediate in the range of values reported for cupredoxins (10^3 to 10^6 M^{-1} sec^{-1}). Plastocyanins from higher plants and green algae have self-exchange rate constants of $\sim 10^3$ M^{-1} sec^{-1} (*126*). These small rate constants are thought to be due to the presence of a large acidic patch on the protein surface, resulting in a large electrostatic repulsion during the self-exchange process. The cupredoxin with the largest self-exchange rate constant is azurin (*127*), which does not have any areas of localized charge on its surface and hence protein–protein association is thought to be facilitated. The intermediate value for amicyanin may reflect the presence of a number of basic residues around the periphery of the hydrophobic patch. The self-exchange rate constant of amicyanin is diminished at lower pH values due to the protonation of His-96 (*110*). This leads to an increased reorganization barrier on going from three-coordinate Cu(I) to four-coordinate Cu(II) and hence the rate of electron transfer is lowered.

e. Mutants. The use of mutagenesis in the study of amicyanin has focused on the active site, with two types of changes made. The first of these involves single mutations of ligating amino acids, whereas the second type has focused on changing a whole ligand-containing loop ("loop-directed mutagenesis"). The axial ligand Met-99 has been replaced with a glutamine (*128*). The identical mutation of the axial Met-121 ligand of azurin has previously been carried out. However, subtle differences exist at the active sites of these two cupredoxins, making the comparison of the effect of the same mutation in the two proteins intriguing. The mutation has a very similar effect in both amicyanin and azurin, with the only difference being a less rhombic EPR spectrum in the former. Both the M99Q

and M121Q mutants of amicyanin and azurin, respectively, are good models for the active site of stellacyanin, which naturally has an axial glutamine ligand.

The replacement of the equatorial ligand His-96 by an aspartate has also been carried out in amicyanin (*129*). The mutant binds Cu(II) to give a variant that is spectroscopically and probably structurally similar to the wild-type protein. The electron self-exchange rate constant of both the M99Q and the H96D amicyanin mutants is considerably diminished, by approximately two orders of magnitude, when compared to the wild-type value of $1.2 \times 10^5\ M^{-1}\ sec^{-1}$. In the case of the H96D mutant it is possible that the efficient electron transfer pathway, involving His-96, has been destroyed. This is further highlighted by the fact that wild-type amicyanin gives a good electrochemical response at a bare glassy carbon electrode but that the H96D mutant does not. An alternative argument could be that in both the H96D and M99Q variants the reorganization energy of the site has been increased by the mutations made.

As mentioned earlier in this section, three of the four active site ligands in cupredoxins are situated close together on a single loop (see Fig. 5). In Table III the loops found in this area of three different cupredoxins are shown. To investigate the role the length and composition of this loop have on the active site properties of amicyanin the corresponding loops from plastocyanin (*113*) and azurin (*130*) have been introduced. The properties of these mutants are compared to wild-type protein in Table IV. In both cases a novel site that is produced does not resemble, spectroscopically, wild-type amicyanin or

TABLE III

C-TERMINAL LIGAND-CONTAINING LOOP OF *Paracoccus versutus* AMICYANIN, POPLAR PLASTOCYANIN, *Alcaligenes faecalis* S-6 PSEUDOAZURIN, AND *Pseudomonas aeruginosa* AZURIN

Protein		Partial C-terminal amino acid sequences													
Amicyanin	93	Cys	Thr	—	Pro	—	His	Pro	—	—	Phe	Met			
Plastocyanin	84	Cys	Ser	—	Pro	—	His	Gln	Gly	Ala	Gly	Met			
Pseudoazurin	78	Cys	Thr	—	Pro	—	His	Tyr	Ala	Met	Gly	Met			
Azurin	112	Cys	Thr	Phe	Pro	Gly	His	Pro	—	Ala	Leu	Met			

TABLE IV

COMPARISON OF THE PROPERTIES OF WILD-TYPE AMICYANIN AND THE PLASTOCYANIN AND AZURIN LOOP MUTANTS

Properties	Wild type	Plastocyanin loop	Azurin loop
Main visible absorption (nm)	596	593	608
$A_{\sim 450}/A_{\sim 600}$	0.10	0.26	0.19
EPR	Axial	Rhombic	Rhombic
Reduction potential (pH 7.0, mV)	234	301	n.d.[a]
Active site pK_a	6.7	5.6	<5.7

[a] n.d., Not determined.

the protein whose active-site loop was introduced. It is also interesting to note that in both cases the pK_a for His-96 is >1 pH unit lower and that the rate of electron self-exchange is diminished.

A final loop-directed mutagenesis experiment carried out on amicyanin involved the introduction of a dinuclear Cu_A center, such as that found in subunit II of CCO (Fig. 9) (*131*). This was achieved by replacing the wild-type loop between Cys-93 and Met-99 with the sequence AEICGPGHSG containing an additional cysteine. The Cu_A variant has spectroscopic properties very similar to those of native Cu_A cen-

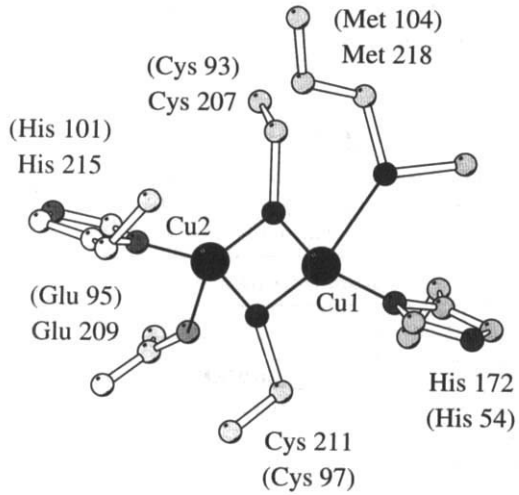

FIG. 9. Representation of the engineered Cu_A site in the soluble domain of subunit II of the bo_3 quinol oxidase from *E. coli* (*37*).

ters (Fig. 10). The paramagnetic form of this mutant has been studied using proton NMR. In this case, as compared to that of wild-type amicyanin (Fig. 11), much sharper isotropically shifted ^1H NMR resonances are observed (*132*), due to much faster electronic spin relaxation. The Fermi-contact shifts have been used to provide detailed information concerning the spin density distribution on the Cu_A ligands. The amount of spin density on the ligands is approximately the same in the Cu_A center as in the mononuclear type 1 site. However, in the former this involves two cysteine and two histidine ligands. The two weak axial interactions at the Cu_A site carry less than 1% spin density and probably have very little covalency. A comparison to the spectrum of the soluble Cu_A domains of the CCOs from *B. subtilis* (*133*) and *P. versutus* (*134*) confirm the similarity of the electronic structure of the Cu_A amicyanin mutant to those of native sites.

2. *Cytochrome* c_{550}

a. Structure. The cytochrome *c* (cyt *c*) component of the MADH redox chain is the monoheme type I cyt c_{550} (also known as cyt c_2). The amino acid sequences of the cyt c_{550}s from *P. versutus* (*135*) and *P. denitrificans* (*136*) are shown in Table V. From this comparison it is clear that there is a strong similarity (84%) between the proteins from these two sources. Cytochrome c_{550} is one of the larger of the bacterial members of this class of metalloproteins and exhibits the highest similarity to the mitochondrial cyt *c* (*137*). A major difference between the bacterial cyt c_{550}s and the mitochondrial cyt *c*s is the presence of a C-terminal 13- to 16-amino-acid-long tail in the former.

The three-dimensional structure of cyt c_{550} from *P. versutus* is not currently available, although NMR studies have provided details of the secondary structure elements plus the dynamic properties of the protein (*138*). The crystal structure of cyt c_{550} from *P. denitrificans* has been reported (*139*) at 1.7 Å resolution (see Fig. 12). The structure shows that the heme group is surrounded by five helices. The protoporphyrin IX ring is covalently attached to the protein via thioether linkages between its vinyl groups and two N-terminal cysteine residues of the protein. Typically, the cysteines are found in the consensus sequence CXXCH. The iron component of the heme is further attached to the protein via two axial ligands: the $N^{\varepsilon 2}$ of His-19 and the S^{δ} of Met-100. The complex environment of the heme in *P. denitrificans* cyt c_{550} also consists of a number of hydrogen bonding interactions involving six water molecules, the side chains of Thr-35, Arg-45, Tyr-55, Trp-71, and Tyr-79, plus a number of protein backbone groups.

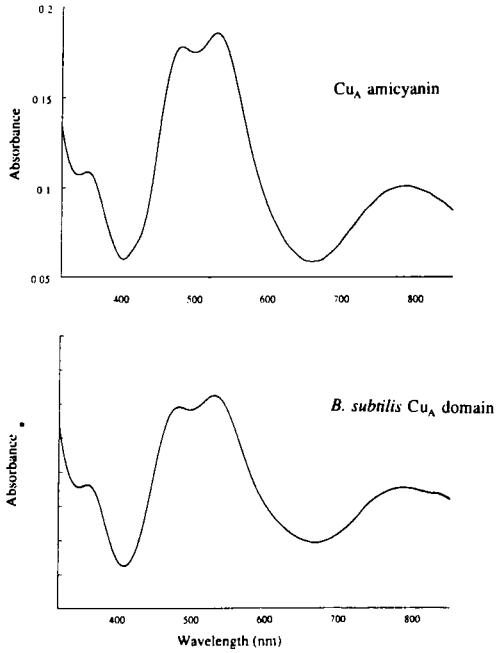
Cu$_A$ amicyanin
Absorbance
0.2
0.15
0.1
0.05
400
500
600
700
800
B. subtilis Cu$_A$ domain
Absorbance
Wavelength (nm)

A

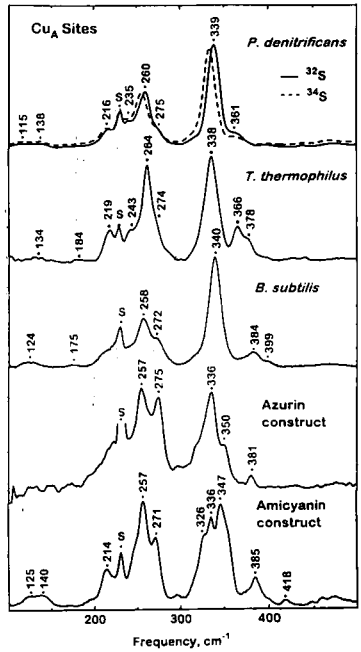
Cu$_A$ Sites
P. denitrificans
^{32}S
^{34}S
115
138
216
235
260
275
339
361
T. thermophilus
134
184
219
243
274
284
338
340
366
378
B. subtilis
124
175
258
272
384
399
Azurin construct
257
275
336
350
361
Amicyanin construct
214
257
271
326
336
347
385
418
200
300
400
Frequency, cm^{-1}

C

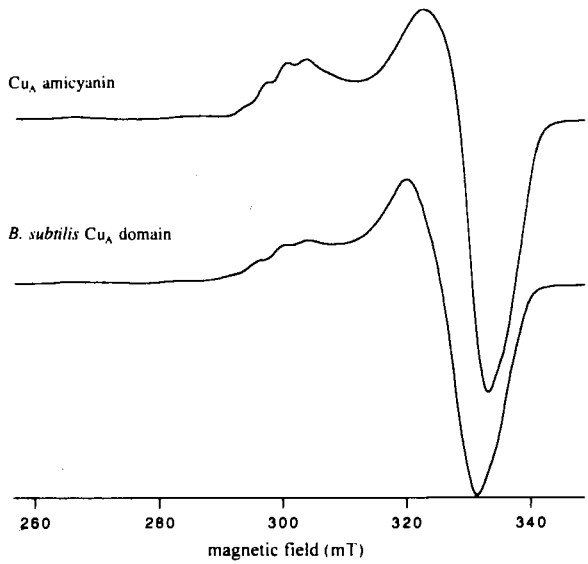
Cu$_A$ amicyanin
B. subtilis Cu$_A$ domain
260
280
300
320
340
magnetic field (mT)

B

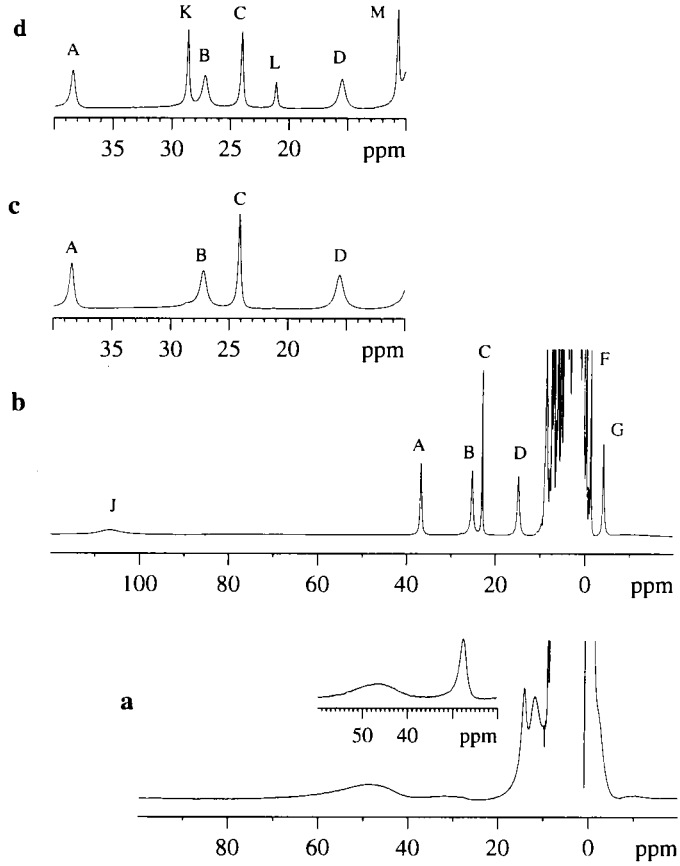

FIG. 11. WEFT spectra of (a) wild-type amicyanin in ^2H_2O at 32°C, with the inset showing the spectrum in H_2O, (b) Cu_A amicyanin in ^2H_2O at 25°C, (c) the region between 40 and 10 ppm in the spectrum of Cu_A amicyanin in ^2H_2O at 7°C, and (d) the same portion of the spectrum of Cu_A amicyanin in H_2O at 7°C.

FIG. 10. Visible spectra of the Cu_A amicyanin variant and the Cu_A domain of COX from *B. subtilis*. (A) The Cu_A amicyanin sample was in HEPES buffer at pH 7.0 whereas the Cu_A domain was in Tris buffer at pH 8.0. (B) The EPR spectra were obtained with the samples at 23 K, with glycereol added as a cryoprotectant. (C) The resonance Raman spectra of Cu_A sites on 488-nm (~150-mW) excitation at 15 K. CCO fragments from *P. denitrificans* (2.0 m*M* in Cu_A), *T. thermophilus* (1.8 m*M* in Cu_A), *B. subtilis* (1.5 m*M* in Cu_A), Cu_A construct in *P. aeruginosa* azurin (~0.4 m*M* in Cu_A), and Cu_A construct in *P. versutus* amicyanin (1.7 m*M* in Cu_A).

TABLE V

COMPARISON OF AMINO ACID SEQUENCES OF CYTOCHROME c_{550} FROM *Paracoccus versutus* AND *Paracoccus denitrificans*[a]

```
Tv    1 MKISIYATLAALSLALPAVA/QEGDAAKGEKEFNKCKACHMVQAPDGTDIV 50
        ***********  ***** * * ****************** ********
Pd    1 MKISIYATLAAITLALPAAA/QDGDAAKGEKEFNKCKACHMIQAPDGTDII 50

Tv   51 KGGKTGPNLYGVVGRKIASVEGFKYGDGILEVAEKNPDMVWSEADLIEYV 100
        ******************** ****** ********** * ********
Pd   51 KGGKTGPNLYGVVGRKIASEEGFKYGEGILEVAEKNPDLTWTEADLIEYV 100

Tv  101 TDPKPWLVEKTGDSAAKTKMTFKLGKNQADVVAFLAQHSPDAGAEA-APA 149
        ********  * *  ******** ************* *****    * *
Pd  101 TDPKPWLVKMTDDKGAKTKMTFKMGKNQADVVAFLAQNSPDAGGDGEAAA 150

Tv  150 EGAAN 154
        **  *
Pd  151 EGESN 155
```

[a] Identical residues are indicated; Tv, *P. versutus* (formerly *Thiobacillus versutus*); Pd, *P. denitrificans*.

Although *P. denitrificans* cyt c_{550} consists of 135 amino acid residues (134 in *P. versutus*), only 122 of these were observed in the crystallographic studies. It has been suggested that this observation is consistent with proteolytic cleavage of the C terminus of the protein, which has also been observed in mass spectroscopic studies on the *P. versutus* protein (*138*). Recent NMR studies on *P. versutus* cyt c_{550} have clearly shown that, in solution, the C terminus of the protein is unstructured and highly mobile, thus making it more prone to proteolysis (*138*).

A common feature of most *c*-type cytochromes is the presence of a ring of basic residues surrounding the exposed heme edge. The center of this ring has a more hydrophobic nature with a conserved phenylalanine residue being found here. Cytochrome c_{550} is no different from the other members of this family in this respect and the role of this surface patch on the electron transfer reactions of the protein will be discussed in subsequent sections of this review.

Cytochrome c_{550} possesses a low-spin iron center (except at extremes of pH values) due to the presence of the axial histidine and methionine ligands (*140*). Therefore, the oxidized form of the protein (Fe^{3+}, d^5) is paramagnetic and the reduced form (Fe^{2+}, d^6) is diamagnetic.

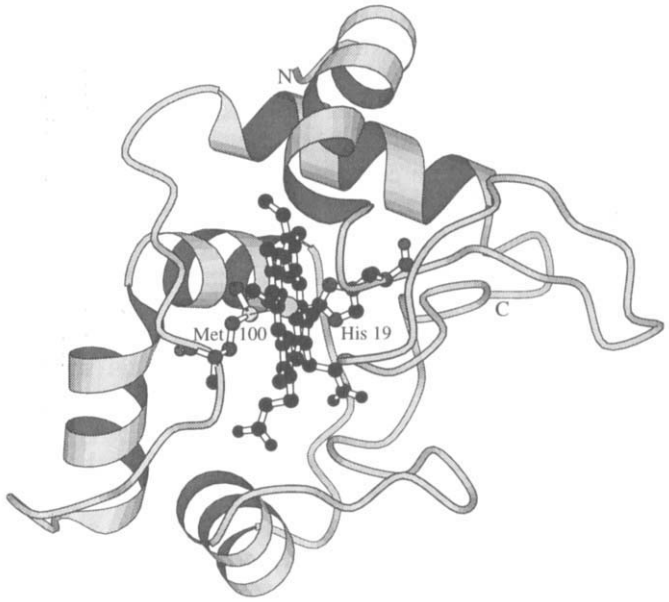

FIG. 12. Ribbon representation of a model of *P. versutus* cyt c_{550} based on the structure of the *P. denitrificans* protein. The heme, axial ligating residues, and His-118 are in ball-and-stick representation. N and C indicate the N and C termini, respectively.

The visible spectrum of the reduced protein is typical of that of a *c*-type cytochrome. The α-band is found at 550 nm, which is utilized in the classification of the protein. On oxidation the α- and β-bands broaden and the intense Soret transition shifts from 416 to 410 nm and its molar absorptivity lowers. An interesting feature of the visible spectrum of the oxidized protein is a weak transition at 696 nm thought to be due to the presence of an axial methionine ligand. The EPR spectrum is typical of a *c*-type cytochrome with values of 1.08, 1.91, and 3.35 for g_x, g_y, and g_z, respectively.

b. pH Effects. At high pH the oxidized form of cyt c_{550} undergoes a number of spectroscopic changes. This is thought to be the result of deprotonation of a lysine residue, which, in its neutral form, replaces the methionine as the axial ligand to the iron (*141*). This conclusion is consistent with the observations that the 696-nm visible absorption band disappears at high pH, and with a decrease in the isotropic shift of the $C^{\varepsilon}H_3$ resonance of the methionine ligand in the ^1H NMR spectrum. In cyt c_{550} the alkaline transition occurs with a pK_a of around 11, whereas in mitochondrial cyt *c* the pK_a is lower, with a value between 9 and 10 typically found (*142*).

A number of mutations have been introduced in *P. versutus* cyt c_{550} in order to investigate the alkaline transition in this protein. The residue Lys-14, which is found in the ring of basic residues surrounding the exposed heme edge, has been replaced with a glutamine and a glutamate (*143*). The rationale behind these changes came from work on horse cyt *c* in which the corresponding Lys-13, which is involved in a salt bridge with Glu-90, was chemically modified with a neutral and a negative group. In both cases a lowering of the pK_a for the alkaline transition of 1 pH unit was observed and was ascribed to the breaking of the salt bridge (*144*). The Lys-14Glu and Lys-14Gln mutants of cyt c_{550} have pK_a values, for the alkaline transition, that are almost identical to that of wild-type protein. This shows that salt bridges made by this residue are not important in maintaining the high pK_a of the alkaline transition in cyt c_{550}.

Various studies on mitochondrial cyt *c* have led to the proposal that two different lysine residues can coordinate to the metal atom, in place of the axial methionine, at alkaline pH values, and site-directed mutagenesis experiments have shown that Lys-79 is one of these (*145*). The corresponding lysine of cyt c_{550} from *P. versutus* (Lys-99) has been replaced with a glutamine (*146*). The effect on the pK_a of the alkaline transition is minimal; the value has lowered by 0.4 pH units to 10.8 in the Lys-99Glu variant. This indicates that the role of this residue in the alkaline transition is not so prominent as in the case of the mitochondrial protein.

A more direct investigation of the alkaline transition of *c*-type cytochromes involved the replacement of the axial Met-100 ligand by a lysine in cyt c_{550}. This produces a variant in which Lys-100 is thought to be the axial ligand and which exhibits spectroscopic properties similar to the alkaline form of cyt *c* (*147*). These spectral features are independent of pH up to a value of 12. Interestingly, the Met-100Lys mutant of cyt c_{550} exhibits certain spectroscopic properties similar to cyt *f*, in which the N terminus of Tyr-1 is known to be one of the axial ligands (*148*).

c. Redox Potential. The reduction potential of cyt c_{550} is typical for this class of heme-containing proteins, and a value of 252 mV in 50 m*M* cacodylate buffer at pH 7 (and at room temperature) has been reported (*147*). The reduction potential of cyt c_{550} is independent of ionic strength but is affected by pH, as shown in Fig. 13. This dependence of the reduction potential on pH is thought to be mainly due to protonation/deprotonation of the heme propionates. Of the mutations made in cyt c_{550}, those at positions 14 and 99 have very little effect on the reduction potential. However, the replacement of the axial methionine ligand with a lysine leads to a drop of approximately 330 mV

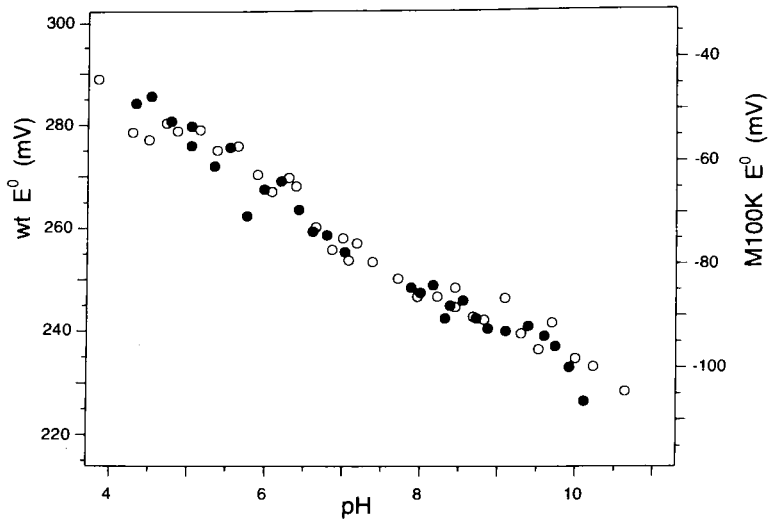

FIG. 13. Midpoint potential (E°) as a function of pH. Data points (±3 mV) were obtained with cyclic voltammetry. Protein concentration was 0.10–0.15 m*M* in 50 m*M* cacodylate/NaOH or HEPES/NaOH buffer. The solid circles and the left *y* axis refer to wild-type cyt c_{550}, whereas the open circles and the right *y* axis are for the M100K cytochrome c_{550} variant.

in the reduction potential. Again, a pH dependence of the reduction potential similar to that in the wild-type protein (Fig. 13) is seen. The drastic effect of the Met-100Lys mutation on the reduction potential of cyt c_{550} is not unexpected, because it gives a potential very similar to that observed for the alkaline form of cyt *c*. Cytochrome *f* has a much higher reduction potential of 365 mV, which is thought to be due to the more buried nature of the heme in this protein (*148*).

d. Electron Self-Exchange. Numerous studies have been made of the self-exchange reactivity of class I *c*-type cytochromes (*149–156*). In most of these it is found that the protein has a low self-exchange rate constant at low ionic strength, which increases as the ionic strength is increased. This behavior is thought to be due to the basic residues that surround the exposed heme edge and prevent efficient protein–protein association. The small (80 amino acid residues) cyt c_{551}s are known to behave differently with respect to self-exchange reactivity. These bacterial proteins have ionic-strength-independent self-exchange rate constants of 10^7 M^{-1} sec^{-1} (*152*). This has been attributed to the smaller number of basic residues around the exposed heme edge of these proteins and to the presence of a larger hydrophobic patch in this area.

Cytochrome c_{550} from *P. versutus* has a self-exchange rate constant (40°C) of $2 \times 10^2\ M^{-1}\ sec^{-1}$ at zero ionic strength and a pH of 6.0 (*143*). The self-exchange rate constant increases by almost three orders of magnitude to $1 \times 10^5\ M^{-1}\ sec^{-1}$ at an ionic strength of 0.55 *M*. The *P. denitrificans* protein appears to be more efficient at self-exchanging, with a reported (*151*) rate constant (25°C) of $1.6 \times 10^4\ M^{-1}\ sec^{-1}$ ($I = 0.1\ M$ and pH 7.5), which compares with a value (40°C) of $4 \times 10^3\ M^{-1}\ sec^{-1}$ for the *P. versutus* protein under similar conditions ($I = 0.1\ M$, pH 6.0). These differences are thought to be due to small structural variations among the two proteins, especially regarding the surface charge properties.

The two mutations at positions 14 of cyt c_{550} from *P. versutus* both have an effect on the self-exchange rate constants (40°C), with values at zero ionic strength of 7×10^3 and $1.2 \times 10^4\ M^{-1}\ sec^{-1}$ reported for the Lys-14Gln and Lys-14Glu variants, respectively (pH 6.0) (*143*). This observation proves the role of the positive area around the heme edge as the recognition site involved in the self-exchange process. It also shows that the removal of a single positive charge in this area favors the formation of an encounter complex and results in a higher second-order self-exchange rate constant.

B. Structure and Function of Methylamine Dehydrogenase and Cytochrome *c* Oxidase

1. *Methylamine Dehydrogenase*

a. Structural Aspects of Methylamine Dehydrogenase. MADH from *P. versutus* is an $\alpha_2\beta_2$ heterotetramer with subunit molecular masses of 47.5 and 12.9 kDa, respectively. The small subunit contains the prosthetic group tryptophan-tryptophyl quinone, which is formed by a 2′–4 covalent cross-link of two tryptophan residues (Trp-57 and Trp-108; see Fig. 14) (*157*). Trp-57 is further modified at positions C-6 and C-7 to yield an orthoquinone structure with $E_{m_7} = 90–100$ mV (*158*).

The three-dimensional structures of MADH from *P. versutus* and *P. denitrificans* have been determined in the presence and absence of amicyanin, and in the presence of amicyanin and cytochrome c_{551i} (*57*, *59–61*, *92*, *159*). The architecture of the tetramer is best described as consisting of two $\alpha\beta$ catalytic units (Fig. 15). Each α-subunit interacts with the β-subunit in the $\alpha\beta$ catalytic units and with the α-subunit of the other $\alpha\beta$ catalytic unit, but there are no interactions between the two β-subunits of the tetramer. The large subunit consists of seven

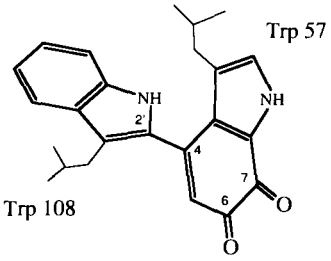

FIG. 14. Structure of the tryptophan-derived TTQ cofactor of MADH. The covalent attachment to the protein through the C^{β} atoms of the modified tryptophans is also shown.

four-stranded antiparallel β-sheets arranged in a circle with a quasi-sevenfold axis. The right-handed twist of these antiparallel β-sheets gives this subunit the appearance of a propeller. The small subunit consists of a central three-stranded β-sheet and some smaller β structures. These β-sheets are connected by long loops and extended regions. The small subunit contains 12 cysteine residues, all of which are involved in disulfide bridge formation, and this extensive cross-linking provides the small subunit with a very rigid structure.

The angle between the planes formed by the indole rings of the TTQ cofactor is approximately 40°, a value similar to that observed by NMR for a TTQ model compound (*161*) and also similar to what has been calculated (*162*). This calculation-based structure suggests that the protein is not a strong determinant of the TTQ conformation. Although the TTQ cofactor, especially the Trp-108 moiety, is located close to the surface of the protein, it interacts via hydrogen bonding with many surrounding residues, all of which (except Phe-64) are derived from the β-subunit (Fig. 16). In fact, all potential H-bond donors and acceptors of the TTQ cofactor participate in H bonding. There is a small pocket near the orthoquinone moiety of Trp-57—involving only C-6 and O-6 and not C-7 and O-7—where substrate and/or ammonia (or water) can bind. Atoms C-5′ and C-6′ of Trp-108 are accessible to solvent but are covered by amicyanin in the MADH–amicyanin complex (at least in *P. denitrificans*) and close to the Cu site. The distance between C-6′ of Trp-108 and the Cu of amicyanin is 9.3 Å; the distance between C-6′ and His-95 of amicyanin only 5.4 Å.

b. Factors Affecting the Structure and Activity of MADH. The pH profile of the reaction catalyzed by MADH is strongly dependent on the type of electron acceptor. Using artificial dyes as electron acceptors, a pH optimum around pH 7.5 occurs, whereas with amicya-

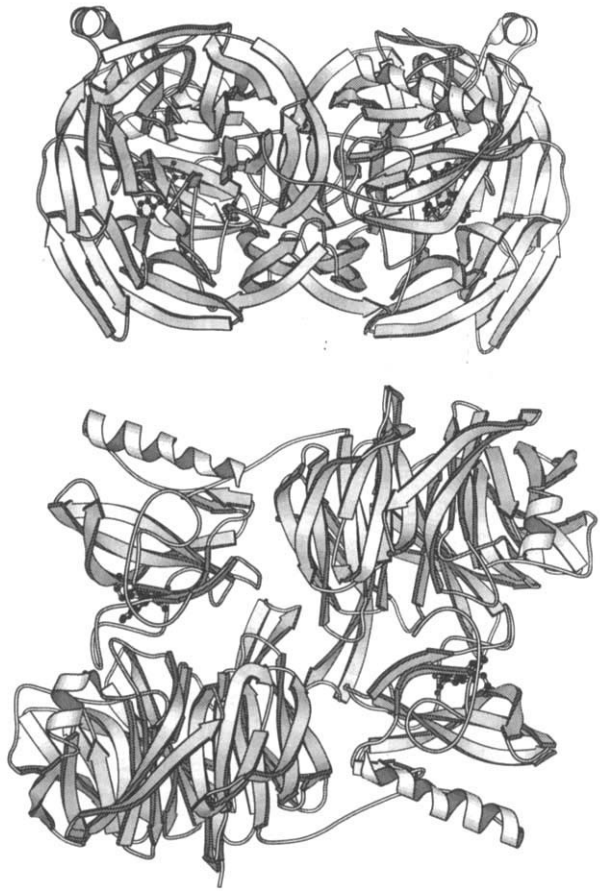

FIG. 15. Representation of the structure of methylamine dehydrogenase based on the crystal structure (*60*, *159*). The secondary structure elements, β-sheets and α-helices, are indicated as plates. The cofactor TTQ is presented in a ball-and-stick form. (Top) This representation shows clearly the small and large subunits, with the extended arm of the large subunit embracing the small subunit. (Bottom) The molecule is turned 90° with respect to the orientation in the top drawing, along the sevenfold symmetry present in the large subunit. A remarkable feature is that the cofactor is located on the extension of this sevenfold axis.

nin no pH optimum is observed (*163*). Furthermore, the absolute turnover number obtained with the natural electron acceptor is much higher (under optimal conditions at 20°C, k_{cat} = 55 electrons/sec) than is obtained with the dyes. As may be expected from products formed in the reaction, both [H^+] and [NH_4^+] have a strong effect on the vari-

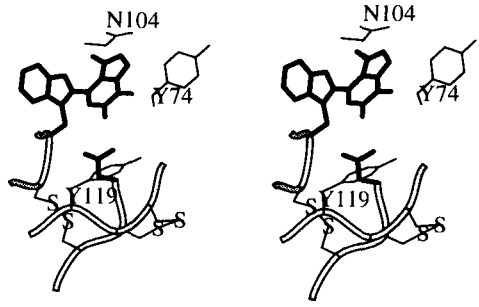

FIG. 16. Stereoview of the TTQ cofactor and surrounding residues. In bold, Trp-108, Trp-59, and Asp-74; disulfide bridges are shown between Cys-109 and Cys-78 (left) and between Cys-77 and Cys-121 (right).

ous steps of the overall reaction. However, other monovalent cations can have similar effects.

The optical spectrum of MADH is largely due to the optical properties of the cofactor TTQ (Fig. 17). Ammonia but also other monovalent cations such as Cs^+, Rb^+, K^+, Na^+, and Li^+, or substrate analogues such as trimethyl- or tetramethylammonia, have a profound effect on the optical spectrum of $MADH_{ox}$, $MADH_{semi}$, and $MADH_{red}$, and also on the activity of the enzyme (*163–165*). To interpret the different effects on the optical spectrum and on the rate of various intermediate steps, it is appropriate to distinguish two types of binding sites for monovalent cations, type I and type II. In the presence of cations such as trimethylammonium and tetramethylammonium, a red shift in the optical spectrum is observed (type I), whereas others (K^+ and Na^+) change the optical spectrum in a manner as observed for reduc-

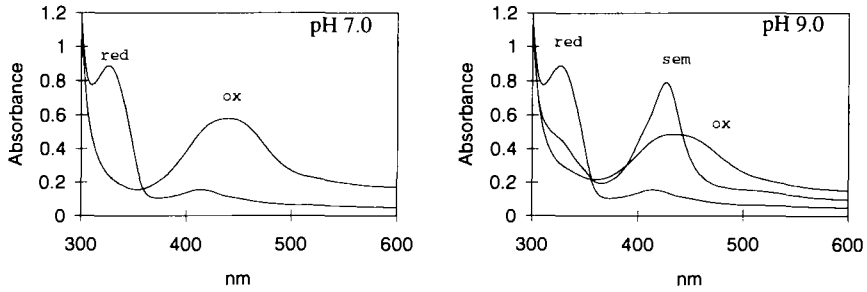

FIG. 17. Left: Absorption spectra of $MADH_{ox}$ and $MADH_{red}$ (obtained with methylamine addition) at pH 7.0. Right: Absorption spectra of the three redox forms of MADH at pH 9.0, the reduced forms being obtained by dithionite addition. The enzyme concentration in both panels is 30 μM.

tion (type II). Cations such as Li^+, Rb^+, Cs^+, and NH_4^+ may bind to both the type I and type II binding sites because they show both optical effects dependent on pH and concentration. Cations binding to the type I binding site compete with the substrate methylamine for binding; binding constants calculated for $MADH_{ox}$ using either an equilibrium binding method or the stopped-flow approach yield the same value. A type I optical spectrum is transiently formed on binding of the substrate.

Resonance Raman spectroscopy suggests a strong electrostatic interaction between type I monovalent cations and the TTQ, but a covalent bond is not formed between the cation and the cofactor (*166*). In particular, an electrostatic interaction with the C-6 carbonyl oxygen atom has been postulated. EPR experiments clearly show strong magnetic coupling between the ^{14}N or ^{15}N nucleus of added NH_4^+ and the electron spin in "dithionite-generated" TTQ_{semi}, but also between the Cs nucleus and TTQ_{semi} (*167*, *168*). Because Cs^+ does not bind covalently to TTQ_{semi}, covalent binding of ammonium or formation of an iminosemiquinone is not a prerequisite to interpret the EPR experiments. In agreement with this is the occurrence of the C-6 oxygen vibration in the resonance Raman spectrum of the dithionite-generated TTQ_{semi} in the presence of added ammonium. In other words, the C-6 oxygen atom is not displaced by NH_4^+ and binding of the cation close to the TTQ_{semi} may be sufficient to elicit the broadening effects seen in EPR.

This latter interpretation is apparently in contradiction to the interpretation given of the electron spin echo envelope modulation (ESEEM) experiments in which TTQ_{semi} had been generated with ^{14}N- or ^{15}N-labeled methylamine (*169*). Like the EPR spectrum, the ESEEM spectrum showed magnetic interaction between the electron spin and the substrate nitrogen. However, the magnitude of the ^{14}N isotropic coupling was proposed to indicate covalent attachment of the substrate nitrogen to the TTQ_{semi}, i.e., the iminosemiquinone had been generated. Recent ESEEM expeiments on the dithionite-generated TTQ_{semi} indicate that this radical is mainly in the anionic form, with the C-6 oxygen forming a hydrogen bond, and further that the angle between the indole ring planes is $48° \pm 11°$ (*170*).

The location of the type II binding site is more difficult to establish. The binding affinity is lower and less specific than for the type I binding site, but in view of the strong negative cooperativity observed between type I and type II cations and the large optical effects displayed, the type II binding site is expected to be close to the TTQ. The monovalent cations not only bind to $MADH_{ox}$ but also to $MADH_{red}$ and

$MADH_{semi}$, as is clear from both optical and EPR spectroscopy. In the presence of Cs^+, Na^+, and NH_4^+, the amount of TTQ semiquinone increases, thus this state is selectively stabilized by these cations. In contrast, trimethylamine binds most strongly to $MADH_{ox}$, does not bind to $MADH_{red}$, and slightly decreases the amount of TTQ_{semi}.

Although k_{cat} and the rate of reduction of TTQ_{ox} by substrate methylamine are practically independent of pH, the rates of other steps show a clear pH dependence and generally increase with increasing pH. For example, the rate of association of methylamine and the specificity constant k_{cat}/K_m for amicyanin are strongly pH dependent. The rate of association of methylamine shows an apparent pK of 8.7 that may be ascribed to the presence of a protonatable group on MADH; methylamine (pK_a = 10.7) is, in this interpretation, assumed to bind as the protonated cation. The pH dependence of the specificity constant for amicyanin can be explained by assuming the presence of two protonatable groups with pK_a values of 6.7 and 8.2. The pK_a value of 6.7 may correspond to the histidine residue, which, when protonated, is responsible for the low rate of the self-exchange reaction of amicyanin. The pK_a of 8.2 may be due to deprotonation of the cation binding site (possibly Asp-76) on the enzyme, similar to what has been concluded on the basis of the optical effects seen for MADH from *P. denitrificans*.

Because TTQ is a two-electron donor and amicyanin is a one-electron acceptor, one can in principle observe two different TTQ-associated oxidation phases, namely, from $TTQ_{red} \rightarrow$ amicyanin and from $TTQ_{semi} \rightarrow$ amicyanin. This is borne out experimentally. The first reaction, $TTQ_{red} \rightarrow$ amicyanin, is much slower than the second, because the TTQ_{semi} form is not normally observed. However, in the presence of monovalent cations the first oxidation step is accelerated much more than the second, consistent with the accumulation of the TTQ_{semi} under these conditions. The monovalent cations do not influence the affinity of amicyanin for MADH but directly affect the rate of electron transfer from the TTQ to the copper site. A semiquantitative analysis suggests that monovalent cations specifically lower the reorganizational barrier (by lowering the value of the reorganization parameter λ (2.2 eV) (cf. *171*) for the first oxidation step somewhat more than for the second, whereas the change in redox midpoint potentials has only a minor effect on the rates.

2. *Cytochrome c Oxidase*

The DNA-derived protein sequence of cytochrome *c* oxidase from *P. versutus* is very similar to that of *P. denitrificans* (*172*). The enzyme

is present in the cytoplasmic membrane of the bacterium and detergents are required for its isolation. To purify the enzyme, the membranes are first preextracted with sodium deoxycholate, which removes loosely bound proteins and the less hydrophobic proteins. Triton X-100 is further used to solubilize the enzyme from *P. versutus*, followed by chromatography on diethylaminoethyl (DEAE) and Q-sepharose columns; a pure enzyme preparation is obtained only after two additional chromatography runs on Mono-Q.

The enzyme purified in Triton X-100 consists of two subunits with apparent molecular masses of 33 and 50 kDa. Its optical spectrum shows features characteristic for cytochrome aa_3: a γ band maximum at 426 nm and an α band maximum at 603 nm for the oxidized enzyme; these values shift to 444 and 605 nm, respectively, for the dithionite-reduced enzyme. The low-temperature EPR spectrum of the oxidized enzyme shows signals originating from low-spin heme *a* ($g_{z,y,x}$ = 2.94, 2.29, 1.39) and from Cu_A (g_z = 2.18 and $g_{x,y} \sim 2.01$). EPR signals from cytochrome a_3 and Cu_B are absent, perhaps due to the antiferromagnetic coupling between these redox centers. The reduced enzyme shows no EPR signals. All these structural and spectroscopic properties are similar to those obtained for the cytochrome aa_3 oxidase from *P. denitrificans* and mitochondrial cytochrome aa_3 oxidases (*173*, *174*).

Optimal activity of the purified enzyme solubilized in Triton X-100 is obtained in the presence of excess phospholipids. The pH optimum of the steady-state reaction with horse heart ferrocytochrome *c* occurs at pH 6, yielding a turnover of about 80 electrons/sec, similar to the value obtained for the enzyme from *P. denitrificans*. Remarkably, a purified membrane-bound *c* cytochrome, identified by its N-terminal sequence as cytochrome c_1 from the bc_1 complex, stimulates the rate of electron transfer between horse heart cytochrome *c* and the cytochrome *c* oxidase by about a factor of two. The *in vitro* enzyme assay with purified cytochrome oxidase and reduced amicyanin showed no activity; only after the addition of endogenous cytochrome c_{550} (or horse heart cytochrome *c*) did oxidation of amicyanin occur, in agreement with the sequence of electron transfer; ami $\rightarrow$ cyt $c_{550} \rightarrow$ CCO.

IV. Electron Transfer Kinetics and Enzymology

A. The Catalytic Cycle of MADH

By analogy with the copper–topaquinone-containing amine oxidase, the catalytic cycle of MADH can be viewed as comprising a reductive

part and an oxidative part (*175*). As discussed above, spectroscopic techniques such as EPR, ESEEM, and resonance Raman spectroscopy indicate that the substrate, or more specifically the ammonium group of the substrate, binds in close vicinity to the TTQ cofactor. Because Cs^+, for example, produces effects in the EPR spectrum of TTQ_{semi} similar to those of ammonia, i.e., hyperfine coupling to the electron spin, the conclusion that these monovalent cations interact electrostatically with TTQ seems justified. However, recent studies have indicated that an iminosemiquinone is probably formed (*177*, *178*). Both alternatives have been incorporated in the scheme of the catalytic cycle depicted in Fig. 18.

As a first step, an electrostatic Michaelis complex is formed (see Fig. 18A) between protonated methylamine and MADH (perhaps involving Asp-76), as evidenced by the transient red shift observed in stopped-flow experiments (*163*). Hereafter, a nucleophilic attack by the amine nitrogen of the substrate takes place at position C-6 of the TTQ cofactor (*159*). The carbinolamine thus formed expells water, leading to the formation of the substrate imine. The expelled water molecule may remain closely bound to the cofactor. The next step is α-proton abstraction (by Asp-76) from the substrate and simultaneous reduction of TTQ, yielding the so-called product imine. Evidence in agreement with proton abstraction (although hydrogen or hydride transfer cannot be ruled out) may come from the large deuterium isotope effect associated with this step (*179–181*). Next is the release of the product formaldehyde; its oxygen atom is proposed to be derived from the enzyme-bound water molecule. At this stage the reductive phase, leading to the formation of the aminophenol intermediate, is completed.

The oxidative phase (see Fig. 18B) consists of two sequential one-electron oxidation reactions with two different amicyanin molecules. On the basis of experiments with apoamicyanin and Zn^{2+}- or Ag^+-substituted amicyanin, one can conclude that oxidized amicyanin has a much higher affinity for MADH than does reduced amicyanin, and further that reduced amicyanin rapidly dissociates from the enzyme (*vide infra*) (*182*). The presence of ammonia or another monovalent cation in the active site promotes rapid oxidation by amicyanin; in particular, the rate of the step from the fully reduced cofactor to the semiquinone state is enhanced (*176*, *183*). It was further observed that the rate of oxidation by amicyanin of the hydroquinone form of TTQ in the absence of NH_4^+ is about 20- to 30-fold lower than the rate of oxidation of the aminophenol (*176*). Nevertheless, whether oxidation of the aminophenol to the iminosemiquinone occurs in the cata-

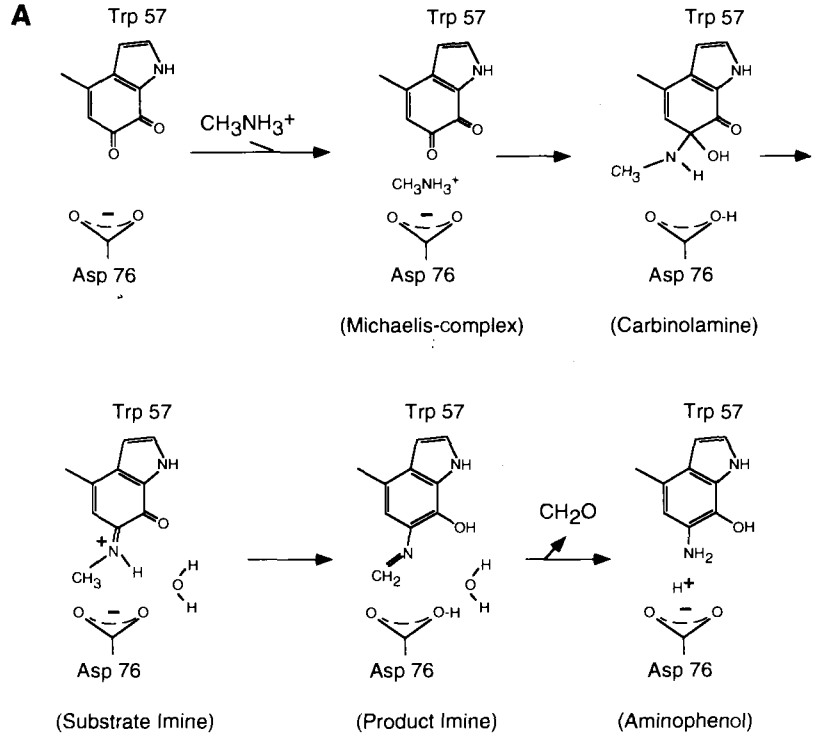

FIG. 18. Catalytic cycle of methylamine dehydrogenase. Both the reductive phase (A) and the oxidative phase (B) are shown; Ami, amicyanin. See text for details.

lytic cycle or during hydration to the hydroquinone form, followed by oxidation to the anionic semiquinone (Fig. 18B), cannot be decided on basis of these latter observations. It is also possible that both reactions may occur. After this step either semiquinone intermediate, or both, may be further oxidized by a second molecule of amicyanin, yielding TTQ_{ox}. In this last step, the monovalent cation NH_4^+ dissociates from MADH, either by itself or as a result of the binding of a substrate molecule, initiating the next catalytic cycle.

B. Reactions between Partners of the MADH Redox Chain

Electron transfer reactions have been investigated only for the first three members of the MADH redox chain from *P. versutus*. In the case of the *P. denitrificans* system extensive studies have been carried out on the reaction between amicyanin and the enzyme MADH (*160*, *171*,

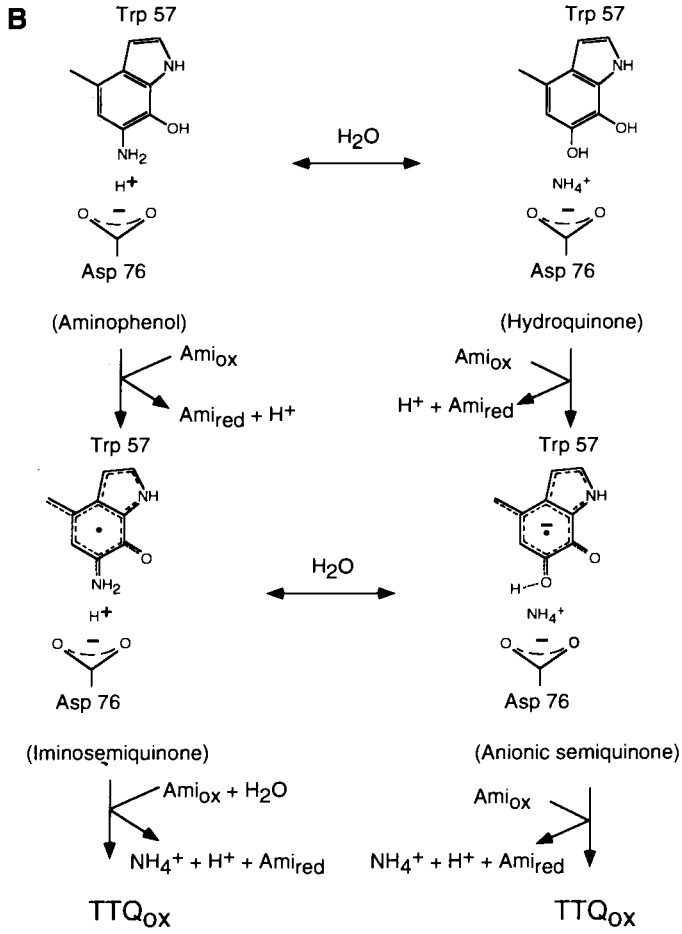

FIG. 18. *Continued*

176, *177*, *184*). The availability of the crystal structure of the binary complex of these two proteins (*92*) adds to the impact of these studies, and provides a model to which current electron transfer theories can be applied. The theoretical results can then be compared with kinetic studies of electron transfer within the complex. Additional studies (*185*, *186*) have focused on the electron transfer reaction between MADH, amicyanin, and cytochrome c_{55li} from *P. denitrificans* (as pointed out in Section II, MADH and amicyanin are induced by growth on methylamine, and cytochrome c_{55li} is induced by growth on methanol). Again, a crystal structure is available for the complex of

these three proteins (*89*, *90*). Studies have also been published on the reaction between cytochrome c_{550} and the Cu_A domain of subunit II of cytochrome *c* oxidase, both from *P. denitrificans* (*187*).

Studies of the *P. versutus* system have concentrated on the nonphysiological electron transfer reaction between MADH and cytochrome c_{550} (*182*). The effects of the Lys-14Gln and Lys-14Glu mutations, at the exposed heme edge of cytochrome c_{550}, on this reaction have been evaluated. Removal of the positive charge at position 14 results in a 20-fold lowering of the second-order rate constant for the reduction of cytochrome c_{550} by MADH. The introduction of a negative charge at this position results in a much larger decrease in the observed rate constant (500-fold). These large effects are not due to alterations in the driving force for the different reactions because the reduction potentials of the two cytochrome c_{550} variants are almost the same as the wild-type value (*vide supra*). Additionally, the two variants both have self-exchange rate constants larger than the wild-type value, and from simple Marcus theory an increase in the rate constant for the cross-reaction with MADH would be expected. These results clearly indicate that the positive charge around the heme edge of cytochrome c_{550} is important for association with a negatively charged region on MADH. Consistent with this observation, the second-order rate constant for the reduction of wild-type cytochrome c_{550} by MADH decreases as the ionic strength is increased.

An extension of the above studies provides a very interesting insight into the interaction between MADH and amicyanin (*182*). Experiments were carried out using redox-inert analogues of oxidized and reduced amicyanin to block the reaction between MADH and cytochrome c_{550}. Zn(II)- and Ag(I)-substituted amicyanin were utilized, and the results of these experiments are shown in Fig. 19. The much greater effect of the Zn(II)–amicyanin on the reaction indicates that the oxidized cupredoxin has a much greater affinity for MADH than does its reduced counterpart. This makes perfect sense in that physiologically oxidized amicyanin needs to associate more strongly with MADH, so that electron transfer can occur. Once the electron has been passed to the copper site the decreased affinity of the reduced protein would facilitate dissociation. Involvement of the protonatable His-96 ligand of amicyanin, which is found in a central position of the interface between the two proteins (see Fig. 20; *vide infra*), is an intriguing option. It has been proposed that once electron transfer from MADH to amicyanin has occurred the histidine ligand will protonate [the pK_a of His-96 in Cu(I) amicyanin is approximately 7; *vide supra*] and thus will aid dissociation (*182*).

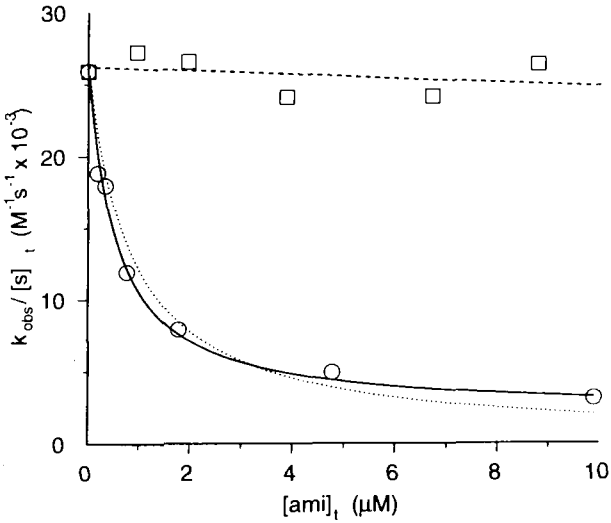

FIG. 19. Inhibition with redox-inactive amicyanins of the oxidation of MADH by cytochrome c_{550}. The circles show the effect of Zn(II)–amicyanin; the squares represent data obtained using Ag(I)–amicyanin (*182*).

The electron transfer reaction between amicyanin and cytochrome c_{550} of *P. versutus* has also been studied (*182a,b*). The effects on this reaction, of the surface mutations to cytochrome c_{550} (K14Q and K14E) and of altering the ionic strength, have been investigated. The results show that oppositely charged surfaces on the two proteins are not utilized in this reaction. This suggests that the basic patch of cytochrome c_{550} is used along with the hydrophobic patch of amicyanin.

Before reviewing the details of the reactions between proteins from *P. denitrificans* it is important to first discuss the available structural information. The proteins MADH and amicyanin are known to associate quite strongly in solution (*188*). A binary complex has been crystallized and the structure (*92*) of part of the interface between the two proteins is shown in Fig. 20. The hydrophobic patch of amicyanin, which surrounds the exposed imidazole ring of the ligand His-96, is found associating with a mainly hydrophobic region on the L subunit of MADH. There are also interactions between amicyanin and the larger H subunit of MADH. The two proteins interact in such a way that the TTQ cofactor of MADH and the copper of amicyanin are approximately 9 Å apart.

A crystal structure is also available for a ternary complex of MADH, amicyanin, and cytochrome c_{551i} (*89*, *90*). The latter protein

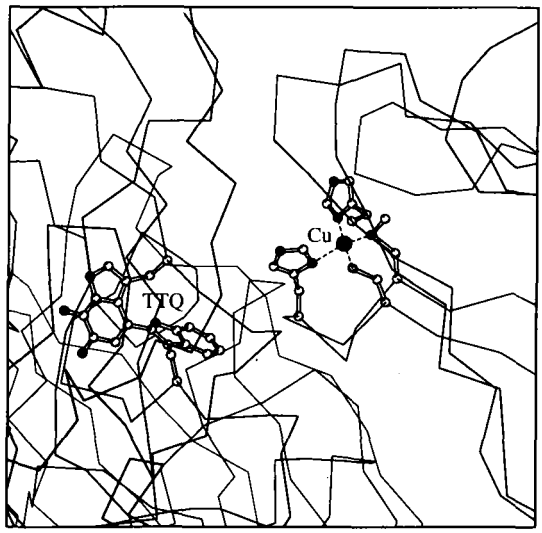

FIG. 20. Position of the TTQ cofactor of MADH and the copper of amicyanin in the crystal structure of the binary complex of the two proteins. The distance from the edge of the TTQ cofactor to the Cu atom is 9.3 Å. The side chain of His-96 is positioned between the Cu and the TTQ. The interface between the two proteins in the complex is formed by the hydrophobic patch of amicyanin and a similar hydrophobic surface of MADH, surrounding the exposed edge of the TTQ cofactor.

is, in fact, the dedicated electron acceptor of the enzyme methanol dehydrogenase (*18*) and the physiological relevance of this complex is at present a matter of debate (see also Section II,A,2). In the ternary complex, MADH and amicyanin associate in almost the same manner as in the binary complex structure. The amicyanin–cytochrome c_{551i} interface in the ternary complex is a lot more polar than that involving MADH and amicyanin. However, the association does not involve oppositely charged surfaces on the two proteins.

Initial studies of the electron transfer reaction between MADH and amicyanin, from *P. denitrificans,* utilized dithionite-reduced MADH (as opposed to the substrate-reduced enzyme). A study of the temperature and driving force dependence of the rate resulted in relatively large calculated values for the reorganization energy (λ) and electronic coupling (H_{AB}) of 2.3 eV and 11.7 cm^{-1}, respectively, for this reaction (*160, 171*). The authors concluded that the electron transfer reaction is coupled to protein rearrangements, and so the observed rate constants contain a contribution from the equilibrium constant for the rearrangement process. It is claimed that the calculated elec-

tronic coupling value is consistent with the distance between the redox cofactors in the binary complex of the proteins. This implies that the crystallographic complex is very similar to that formed in solution. A direct distance of 7.8 Å was derived using a β (electronic decay factor) value of 1.4 $Å^{-1}$, whereas a through-bond path length of 12.4 Å was predicted using a β value of 0.7 $Å^{-1}$. The direct distance between the TTQ cofactor of MADH and the copper of amicyanin is 9.4 Å, whereas a pathway analysis provided a route of 14 Å, including a 3.6-Å through-space jump.

As explained in detail above, the reduction of MADH by its physiological substrate (methylamine) is believed to result in the formation of an aminophenol form of the TTQ cofactor. Subsequent one-electron oxidation of MADH leads to the formation of an aminosemiquinone TTQ intermediate, and finally, following a second electron transfer step, to the quinone TTQ resting state of the enzyme (*176–178*). The temperature dependence of the rate constants observed for the oxidation of methylamine-reduced MADH by amicyanin provides values of λ (3.53 eV) and H_{AB} (22,850 cm^{-1}) that are physically meaningless. This indicates that the reaction is gated, i.e., the observed rate constant does not describe electron transfer. To further investigate the cause of gating, the oxidation of both dithionite- and methylamine-reduced MADH, by amicyanin, was studied in deuterated solvent (*176*). The observation of a large solvent (D_2O/H_2O) kinetic isotope effect for the reaction involving methylamine-reduced MADH, and not for the dithionite-reduced protein, clearly indicates that the adiabatic process that gates electron transfer involves the transfer of an exchangeable proton.

The question of the physiological significance of the crystal structure of the ternary complex of MADH, amicyanin, and the cytochrome c_{551i} from *P. denitrificans* has already been mentioned. The argument used in favor of this structure being physiologically relevant is that, *in vitro,* cytochrome c_{551i} is the most efficient electron acceptor for the MADH–amicyanin complex, of three *c*-type cytochromes found in *P. denitrificans* (*63*). However, the fact that cytochrome c_{551i} is the dedicated electron acceptor of the enzyme methanol dehydrogenase (*18*) would, intuitively, argue against this proposal. Additionally, a mutant strain of *P. denitrificans* in which the cytochrome c_{551i} gene has been knocked out exhibited growth characteristics, on methylamine, identical to the wild-type strain. A different mutant strain, with the cytochrome c_{550} gene knocked out, showed a decrease in the maximum specific growth rate on methylamine. Nevertheless, the Davidson group has carried out extensive studies on the electron

transfer reactions between MADH, amicyanin, and cytochrome c_{551i}. Polarized absorption spectroscopy has been utilized (*189*) to demonstrate that the crystallographic complexes (binary and ternary) are both capable of methylamine oxidation. In the ternary complex the subsequent reduction of the heme of cytochrome c_{551i} occurs in about 35 min at pH 9.0. Interestingly, the reduction of heme still occurs in crystals containing apoamicyanin, but in that case takes approximately 4 days (at pH 7.5). It should be noted that in all cases a pH dependence of the rate of electron transfer from MADH is observed, with faster rates obtained at the more alkaline pH values. This has been attributed either to the protonation of the His-95 ligand of amicyanin at lower pH values (*vide supra*) and/or to the stabilization of the TTQ aminosemiquinone at high pH.

Studies in solution of the reaction between the MADH–amicyanin complex and cytochrome c_{551i} have been interpreted in the following way. It is believed that the association of amicyanin with MADH leads to a lowering of the reduction potential of the amicyanin by 73 mV, to a value of 221 mV (at pH 7.5) (*184*) (this assumption was also made in the analysis of the MADH–amicyanin kinetics). This makes electron transfer to cytochrome c_{551i}, which has a reduction potential of 190 mV (*190*), more favorable. This proposal has been questioned (*182a*), and it has been suggested that the observed differences between the reduction potential of free amicyanin and amicyanin complexed to MADH reflect nothing more than the different affinities of oxidized and reduced amicyanin for MADH, which was not taken into account in the interpretation of the spectroelectrochemical data (*184*). Another assumption that has been made in the interpretation of the kinetics of this reaction is that amicyanin complexed to MADH is solely responsible for the observed reduction of cytochrome c_{551i}. The reduction of cytochrome c_{551i} by free amicyanin, although thermodynamically unfavorable, occurs too quickly to be monitored by the technique used (*184*). This indicates that the interaction of free amicyanin and cytochrome c_{551i} allows the two proteins to associate in a way that enhances the electronic coupling between the two metal centers. Alternatively, the faster reaction could be due to an enhanced association constant for the two proteins in the absence of MADH.

More detailed electron transfer studies indicate that cytochrome c_{551i} and the MADH–amicyanin complex associate in solution (*186*). The temperature dependence of the rate constant for electron transfer from copper to iron, within this ternary complex, provides estimates of λ and H_{AB} of 1.1 eV and 0.3 cm^{-1}, respectively. These results are consistent with electron transfer over distances of 13–23 Å, de-

pending on the β value used. This appears to agree with a direct copper-to-iron distance of 24.7 Å (the copper-to-heme edge distance is 22.7 Å) in the ternary complex. Again these results are used to imply that the arrangement of the proteins seen in the crystallographic studies is also relevant in solution.

Extensive mutagenesis studies have been used to investigate the interaction between cytochrome c_{550} and the soluble Cu_A domain of subunit II of cytochrome *c* oxidase (both proteins from *P. denitrificans*) (*187*). Removal of acidic residues on the surface of the Cu_A domain, close to the metal site, results in a decrease in the second-order rate constant for the oxidation of cytochrome c_{551i}. This indicates that the acidic patch on the Cu_A domain of cytochrome *c* oxidase is used for association with the basic patch of cytochrome c_{550}. Similar studies have also been carried out on the complete oxidase from *P. denitrificans* utilizing, in this case, horse heart cytochrome *c* as the electron donor (*191*). Again the importance of the acidic residues of subunit II of the oxidase, for this interaction, was demonstrated.

Acknowledgments

The authors thank Petra van Bastelaere, Ilaria Ciabatti, and Gertrüd Warmerdam for providing information on the protein chemistry of cytochrome oxidase of *P. versutus* and the DNA sequence of the COX-encoding gene of *P. versutus*. Thanks to Rutger Diederix, Lars Jeuken, and Aldo J. Jongejan for help with producing the figures. Parts of the work were supported by the European Community under the HCMP network (CHRX-CT93-0189) and by the foundation for chemical research (SON) under the auspices of the Netherlands Science Organization (NWO).

References

1. Katayama, Y.; Hiraishi, A.; Kuraishi, H. *Microbiology* **1995,** *141,* 1469.
2. Beijerinck, M.; Minkman, D. C. J. *Zentralbl. Bakteriol. Parasitenik. Abt. II* **1910,** *25,* 30.
3. Goodhew, C. F.; Pettigrew, G. W.; de Vreese, B.; van Beeumen, J.; van Spanning, R. J. M.; Baker, S. C.; Saunders, N.; Ferguson, S. J.; Thompson, I. P. *FEMS Microbiol. Lett.* **1996,** *137,* 95.
4. Woese, C. R. *Microbiol. Rev.* **1987,** *51,* 221.
5. Bosma, G.; Braster, M.; Stouthamer, A. H.; van Verseveld, H. W. *Eur. J. Biochem.* **1987,** *165,* 665.
6. Bosma, G.; Braster, M.; Stouthamer, A. H.; van Verseveld, H. W. *Eur. J. Biochem.* **1987,** *165,* 657.
7. van der Oost, J.; de Boer, A. P. N.; de Gier, J.-W. L.; Zumft, W. G.; Stouthamer, A. H.; van Spanning, R. J. M. *FEMS Microbiol. Lett.* **1994,** *121,* 1.

8. van Spanning, R. J. M.; de Boer, A. P. N.; Reijnders, W. N. M.; de Gier, J. W. L.; Delorme, C. O.; Stouthamer, A. H.; Westerhoff, H. V.; Harms, N.; van der Oost, J. *J. Bioenerg. Biomembr.* **1995,** *27,* 499.
9. van Verseveld, H. W.; Stouthamer, A. H. "The Genus *Paracoccus*"; The Prokaryotes, 2nd Ed.; Balows, Trupes, Dworkin, Hardev, and Scleifer, Eds.; Springer-Verlag, New York, 1991; pp. 2321–2334.
10. Stouthamer, A. H. *J. Bioenerg. Biomembr.* **1991,** *23,* 163.
11. Stouthamer, A. H. *Anton Leeuwenhoek Int. J. Gen. Microbiol.* **1992,** *61,* 1.
12. de Gier, J. W. L.; Lubben, M.; Reijnders, W. N. M.; Tipker, C. A.; Slotboom, D. J.; van Spanning, R. J. M.; Stouthamer, A. H.; van der Oost. J. *Mol. Microbiol.* **1994,** *13,* 183.
13. de Gier, J. W. L.; van der Oost, J.; Harms, N.; Stouthamer, A. H.; van Spanning, R. J. M. *Eur. J. Biochem.* **1995,** *229,* 148.
14. Harms, N.; Reijnders, W. N. M.; Anazawa, H.; van der Palen, C. J. N. M.; van Spanning, R. J. M.; Oltmann, L. F.; Stouthamer, A. H. *Mol. Microbiol.* **1993,** *8,* 457.
15. van Spanning, R. J. M.; van der Palen, C. J. N. M.; Slotboom, D. J.; Reijnders, W. N. M.; Stouthamer, A. H.; Duine, J. A. *Eur. J. Biochem.* **1994,** *226,* 201.
16. van Spanning, R. J. M.; de Boer, A. P. N.; Reijnders, W. N. M.; Spiro, S.; Westerhoff, H. V.; Stouthamer, A. H.; van der Oost, J. *FEBS Lett.* **1995,** *360,* 151.
17. van Spanning, R. J. M.; Wansell, C. W.; Harms, N.; Oltmann, L. F.; Stouthamer, A. H. *J. Bacteriol.* **1990,** *172,* 986.
18. van Spanning, R. J. M.; Wansell, C. W.; Reijnders, W. N. M.; Harms, N.; Ras, J.; Oltmann, L. F.; Stouthamer, A. H. *J. Bacteriol.* **1991,** *173,* 6962.
19. Harms, N.; van Spanning, R. J. M. *J. Bioenerg. Biomembr.* **1991,** *23,* 187.
20. Albracht, S. P. J.; van Verseveld, H. W.; Hagen, R. H.; Kalkman, M. L. *Biochim. Biophys. Acta.* **1980,** *593,* 173.
21. John, P.; Whatley, F. R. *Nature* **1975,** *254,* 495.
22. Bosma, G. Ph.D. thesis, 1989; Vrije Universiteit, Amsterdam.
23. van Verseveld, H. W.; Braster, M.; Boogerd, F. C.; Chance, B.; Stouthamer, A. H. *Arch. Microbiol.* **1983,** *135,* 229.
24. van Spanning, R. J. M. Ph.D. thesis, Vrÿe Universiteit, Amsterdam, The Netherlands, 1991.
25. van Verseveld, H. W.; Stouthamer, A. H. *Arch. Microbiol.* **1978,** *118,* 13.
26. van Verseveld, H. W. Stouthamer, A. H. *Arch. Microbiol.* **1978,** *118,* 21.
27. Garciahorsman, J. A.; Berry, E.; Shapleigh, J. P.; Alben, J. O.; Gennis, R. B. *Biochemistry* **1994,** *33,* 3113; Garciahorsman, J. A.; Barquera, B.; Rumbley, J.; Ma, J. X.; Gennis, R. B. *J. Bacteriol.* **1994,** *176,* 5587.
28. Castresana, J.; Lubben, M.; Saraste, M. *J. Mol. Biol.* **1995,** *250,* 202.
29. Saraste, M.; Castresana, J. *FEBS Lett.* **1994,** *341,* 1.
30. Brown, S.; Moody, A. J.; Mitchell, R.; Rich, P. R. *FEBS Lett.* **1993,** *316,* 216.
31. Hosler, J. P.; Fergusonmiller, S.; Calhoun, M. W.; Thomas, J. W.; Hill, J.; Lemieux, L.; Ma, J. X.; Georgiou, C.; Fetter, J.; Shapleigh, J.; Tecklenburg, M. M. J.; Babcock, G. T.; Gennis, R. B. *J. Bioenerg. Biomembr.* **1993,** *25,* 121.
32. Babcock, G. T.; Wikstrom, M. *Nature* **1992,** *356,* 301.
33. Iwata, S.; Ostermeier, C.; Ludwig, B.; Michel, H. *Nature* **1995,** *376,* 660.
34. Kleymann, G.; Ostermeier, C.; Ludwig, B.; Skerra, A.; Michel, H. *Biotechnology* **1995,** *13,* 155.
35. de Gier, J. W. L.; Schepper, M.; Reijnders, W. N. M.; van Dyck, S. J.; Slotboom, D. J.; Warne, A.; Saraste, M.; Krab, K.; Finel, M.; Stouthamer, A. H.; van Spanning, R. J. M.; van der Oost, J. *Mol. Microbiol.* **1996,** *20,* 1247.

36. Hill, B. C. *J. Bioenerg. Biomembr.* **1993,** *25,* 115.
37. Wilmanns, M.; Lappalainen, P.; Kelly, M.; Sauereriksson, E.; Saraste, M. *Proc. Natl. Acad. Sci. U.S.A.* **1995,** *92,* 11955.
38. Chepuri, V.; Lemieux, L.; Au, D. C.-T.; Gennis, R. B. *J. Biol. Chem.* **1990,** *265,* 11185.
39. Mandon, K.; Kaminski, P. A.; Elmerich, C. *J. Bacteriol.* **1994,** *176,* 2560.
40. Thonymeyer, L.; Beck, C.; Preisig, O.; Hennecke, H. *Mol. Microbiol.* **1994,** *14,* 705.
41. Preisig, O.; Zufferey, R.; Thonymeyer, L.; Appleby, C. A.; Hennecke, H. *J. Bacteriol.* **1996,** *178,* 1532.
42. Preisig, O.; Anthamattan, D.; Hennecke, H. *Proc. Natl. Acad. Sci. U.S.A.* **1993,** *90,* 3309.
43. Kahn, D.; Batut, J.; Daveran, M.-L.; Fourment, J. In "New Horizons in Nitrogen Fixation"; Palacios, R. J., Mora, W. E., and Newton, W. E., Eds.; Kluwer Academic: Dordrecht, The Netherlands, 1993; p. 474.
44. Richter, O. M. H.; Tao, J. S.; Turba, A.; Ludwig, B. *J. Biol. Chem.* **1994,** *269,* 23079.
45. Berks, B. C.; Ferguson, S. J.; Moir, J. W. B.; Richardson, D. J. *Biochim. Biophys. Acta Bioenergetics* **1995,** *1232,* 97.
46. Ferguson, S. J. *Anton Leeuwenhoek Int. J. Gen. Microbiol.* **1994,** *66,* 89.
47. van Spanning, R. J. M.; de Boer, A. P. N.; Reijnders, W. N. M.; Stouthamer, A. H.; Westerhoff, H. V.; van der Oost, J. *Molec. Microbiol.* **1996,** *23,* 893.
48. Friedrich, C. G.; Mitrenga, G. *FEMS Microbiol. Lett.* **1981,** *10,* 209.
49. Wodara, C.; Kostka, S.; Egert, M.; Kelly, D. P.; Friedrich, C. G. *J. Bacteriol.* **1994,** *176,* 6188.
50. John, P.; Whatley, F. R. *Biochim. Biophys. Acta* **1977,** *463,* 129.
51. van Spanning, R. J. M.; Wansell, C. W.; de Boer, T.; Hazelaar, M. J.; Anazawa, H.; Harms, N.; Oltmann, L. F.; Stouthamer, A. H. *J. Bacteriol.* **1991,** *173,* 6948.
52. Anthony, C.; Ghosh, M.; Blake, C. C. F. *Biochem. J.* **1994,** *304,* 665.
53. Blake, C. C. F.; Ghosh, M.; Harlos, K.; Avezoux, A.; Anthony, C. *Nature Struct. Biol.* **1994,** *1,* 102.
54. Anthony, C. *Adv. Microb. Physiol.* **1986,** *27,* 113.
55. Lidstrom, M. E.; Anthony, C.; Biville, F.; Gasser, F.; Goodwin, P.; Hanson, R. S.; Harms, N. *FEMS Microbiol. Lett.* **1994,** *117,* 103.
56. Chistoserdov, A. Y.; Chistoserdova, L. V.; Mcintire, W. S.; Lidstrom, M. E. *J. Bacteriol.* **1994,** *176,* 4052.
57. Chistoserdov, A. Y.; Boyd, J.; Mathews, F. S.; Lidstrom, M. E. *Biochem. Biophys. Res. Commun.* **1992,** *184,* 1226.
58. van der Palen, C. J. N. M.; Slotboom, D. J.; Jongejan, L.; Reijnders, W. N. M.; Harms, N.; Duine, J. A.; van Spanning, R. J. M. *Eur. J. Biochem.* **1995,** *230,* 860.
59. Chen, L.; Mathews, F. S.; Davidson, V. L.; Huizinga, E. G.; Vellieux, F. M. D.; Hol, W. G. J. *Proteins: Struct. Funct. Genet.* **1992,** *14,* 288.
60. Vellieux, F. M. D.; Huitema, F.; Groendijk, H.; Kalk, K. H.; Frank, J.; Jongejan, J.; Duine, J. A.; Petratos, K.; Drenth, J.; Hol, W. G. J. *EMBO J.* **1989,** *8,* 2171.
61. Chen, L.; Mathews, F. S.; Davidson, V. L.; Huizinga, E. G.; Vellieux, F. M. D.; Duine, J. A.; Hol, W. G. J. *FEBS Lett.* **1991,** *287,* 163.
62. Husain, M.; Davidson, V. L. *J. Biol. Chem.* **1985,** *260,* 14626.
63. van Spanning, R. J. M.; Wansell, C. W.; Reijnders, W. N. M.; Oltmann, L. F.; Stouthamer, A. H. *FEBS Lett.* **1990,** *275,* 217.
64. Gak, E. R.; Chistoserdov, A. Y.; Lidstrom, M. E. *J. Bacteriol.* **1995,** *177,* 4575.
65. Burton, S. M.; Byrom, D.; Carver, M.; Jones, G. D. D.; Jones, C. W. *FEMS Microbiol. Lett.* **1983,** *17,* 185.

66. Chandrasekar, R.; Klapper, M. H. *J. Biol. Chem.* **1986,** *261,* 3616.
67. Husain, M.; Davidson, V. L. *J. Biol. Chem.* **1986,** *261,* 8577.
68. Ras, J.; Reijnders, W. N. M.; van Spanning, R. J. M.; Harms, N.; Oltmann, L. F.; Stouthamer, A. H. *J. Bacteriol.* **1991,** *173,* 6971.
69. Kostler, M.; Kleiner, D. *FEMS Microbiol. Lett* **1989,** *65,* 1.
70. van Ophem, P. W.; Duine, J. A. *FEMS Microbiol. Lett.* **1994,** *116,* 87.
71. Harms, N.; Ras, J.; Reijnders, W. N. M.; van Spanning, R. J. M.; Stouthamer, A. H. *J. Bacteriol.* **1996,** *178,* 6296.
72. Ras, J.; van Ophem, P. W.; Reijnders, W. N. M.; van Spanning, R. J. M.; Duine, J. A.; Stouthamer, A. H.; Harms, N. *J. Bacteriol.* **1995,** *177,* 247.
73. Harms, N. Ph.D. Thesis, Vrije Universiteit, Amsterdam, The Netherlands, 1988.
73a. Ubbink, M.; van Kleef, M. A. G.; Kleinjan, D.-J.; Hoitink, C. W. G.; Huitema, F.; Beintema, J. J.; Duine, J. A.; Canters, G. W. *Eur. J. Biochem.* **1991,** *202,* 1003.
74. Husain, M.; Davidson, V. L. *J. Bacteriol.* **1987,** *169,* 1712.
75. Harms, N.; Ras, J.; Koning, S.; Reijnders, W. N. M.; Stouthamer, A. H.; van Spanning, R. J. M. In "Microbial Growth on C1 Compounds"; Lidstrom, M. E., and Tabita, F. R., Eds.; Kluwer Academic: Dordrecht, The Netherlands, 1995; pp. 126–132.
76. Parkinson, J. S. *Cell* **1993,** *73,* 857.
77. Yang, H.; Reijnders, W. N. M.; van Spanning, R. J. M.; Stouthamer, A. H.; Harms, N. *Microbiology* **1995,** *141,* 825.
78. Xu, H. H.; Janka, J. J.; Viebahn, M.; Hanson, R. S. *Microbiology* **1995,** *141,* 2543.
79. Schell, M. A. *Annu. Rev. Microbiol.* **1993,** *47,* 597.
80. (a) Delorme, C.; Huisman, T. T.; Reijnders, W. N. M.; Chan, Y.-L.; Harms, N.; Stouthamer, A. H.; van Spanning, R. J. M. *Microbiology* **1997,** *143,* 793; (b) Parsek, M. R.; Ye, R. W.; Pun, P.; Chakrabarty, A. M. *J. Biol. Chem.* **1994,** *269,* 11279.
81. Huitema, F.; van Beeumen, J.; van Driessche, G.; Duine, J. A.; Canters, G. W. *J. Bacteriol.* **1993,** *175,* 6254.
82. Gunsalus, R. P.; Park, S. J. *Res. Microbiol.* **1994,** *145,* 437.
83. Spiro, S. *Anton Leeuwenhoek Int. J. Gen. Microbiol.* **1994,** *66,* 23.
84. Khoroshilova, N.; Beinert, H.; Kiley, P. J. *Proc. Natl. Acad. Sci. U.S.A.* **1995,** *92,* 2499.
85. Stoll, R.; Page, M. D.; Sambongi, Y.; Ferguson, S. J. *Microbiology* **1996,** *142,* 2577.
86. van Spanning, R. J. M.; Wansell, C. W.; Reijnders, W. N. M.; Oltmann, L. F.; Stouthamer, A. H. *FEBS Lett.* **1990,** *275,* 217.
87. van Beeumen, J.; van Bun, S.; Canters, G. W.; Lommen, A.; Chothia, C. *J. Biol. Chem.* **1991,** *266,* 4869.
88. Romero, A.; Nar, H.; Messerschmidt, A.; Kalverda, A. P.; Canters, G. W.; Durley, R.; Mathews, F. S. *J. Mol. Biol.* **1994,** *236,* 1196.
89. Kalverda, A. P.; Wymenga, S. S.; Lommen, A.; van de Ven, F. J. M.; Hilbers, C. W.; Canters, G. W. *J. Mol. Biol.* **1994,** *240,* 358.
90. Durley, R.; Chen, L.; Lim, L. W.; Mathews, F. S. *Protein Sci.* **1993,** *2,* 739.
91. Cunane, L. M.; Chen, Z.; Durley, R. C. E.; Mathews, F. S. *Acta Crystallogr.* **1996,** *D52,* 676.
92. Chen, L.; Durley, R.; Poliks, B. J.; Hamada, K.; Chen, Z.; Mathews, F. S.; Davidson, V. L.; Satow, Y.; Huizinga, E.; Vellieux, F. M. D.; Hol, W. G. J. *Biochemistry* **1992,** *31,* 4959.
93. Chen, L.; Mathews, F. S.; Davidson, V. L.; Tegoni, M.; Rivetti, C.; Rossi, G. L. *Protein Sci.* **1993,** *2,* 147.
94. Chen, L.; Durley, R. C. E.; Mathews, F. S.; Davidson, V. L. *Science* **1994,** *264,* 86.

95. Walter, R. L.; Ealick, S. E.; Friedman, A. M.; Blake, R. C.; Proctor, P.; Shoham, M. *J. Mol. Biol.* **1996,** *263,* 730.
96. Botuyan, M. V.; Toy-Palmer, A.; Chung, J.; Blake, R. C.; Beroza, P.; Case, D.; Dyson, H. *J. Mol. Biol.* **1996,** *263,* 752.
97. Han, J.; Loehr, T. M.; Lu, Y.; Valentine, J. S.; Averill, B. A.; Sanders-Loehr, J. *J. Am. Chem. Soc.* **1993,** *115,* 4256.
98. Canters, G. W.; Gilardi, G. *FEBS Lett.* **1993,** *325,* 39.
99. LaCroix, L. B.; Shadle, S. E.; Wang, Y.; Averill, B. A.; Hedman, B.; Hodgson, K. O.; Solomon, E. I. *J. Am. Chem. Soc.* **1996,** *118,* 7755.
100. van Houwelingen, T.; Canters, G. W.; Stobbelaar, G.; Duine, J. A.; Frank, J.; Tsugita, A. *Eur. J. Biochem.* **1985,** *153,* 75.
101. Husain, M.; Davidson, V. L.; Smith, A. J. *Biochemistry* **1986,** *25,* 2431.
102. Adman, E. T.; Godden, J. W.; Turley, S. J. *J. Biol. Chem.* **1995,** *270,* 27458.
103. Guss, J. M.; Merritt, E. A.; Phizackerley, R. P.; Freeman, H. C. *J. Mol. Biol.* **1996,** *262,* 686.
104. Petratos, K.; Dauter, Z.; Wilson, K. S. *Acta Crystallogr.* **1988,** *B44,* 628.
105. Adman, E. T.; Turley, S.; Bramson, R.; Petratos, K.; Banner, D.; Tsneroglou, D.; Beppu, T.; Watanabe, H. *J. Biol. Chem.* **1989,** *264,* 87.
106. Andrew, C. R.; Yeom, H.; Valentine, J. S.; Karlsson, B. G.; Bonander, N.; van Pouderoyen, G.; Canters, G. W.; Loehr, T. M.; Sanders-Loehr, J. *J. Am. Chem. Soc.* **1994,** *116,* 11489.
107. Andrew, C. R.; Sanders-Loehr, J. *Acc. Chem. Res.* **1996,** *29,* 365.
108. Kalverda, A. P.; Salgado, J.; Dennison, C.; Canters, G. W. *Biochemistry* **1996,** *35,* 3085.
109. Lommen, A.; Canters, G. W.; van Beeuman, J. *Eur. J. Biochem.* **1988,** *176,* 213.
110. Lommen, A.; Canters, G. W. *J. Biol. Chem.* **1990,** *265,* 2768.
111. Lommen, A.; Pandya, K. I.; Koningsberger, D. C.; Canters, G. W. *Biochim. Biophys. Acta* **1991,** *1076,* 439.
112. Kyritsis, P.; Dennison, C.; Kalverda, A. P.; Canters, G. W.; Sykes, A. G. *J. Chem. Soc., Dalton Trans.* **1994,** *3017.*
113. Dennison, C.; Vijgenboom, E.; Hagen, W. R.; Canters, G. W. *J. Am. Chem. Soc.* **1996,** *118,* 7406.
114. Segal, M. G.; Sykes, A. G. *J. Am. Chem. Soc.* **1978,** *100,* 4584.
115. Sykes, A. G. *Chem. Soc. Rev.* **1985,** *14,* 283.
116. Sykes, A. G. *Adv. Inorg. Chem.* **1991,** *36,* 377.
117. Guss, J. M.; Harrowell, P. R.; Murata, M.; Norris, V. A.; Freeman, H. C. *J. Mol. Biol.* **1986,** *192,* 361.
118. Kojiro, C. L.; Markley, J. L. *FEBS Lett.* **1983,** *162,* 52.
119. Dennison, C.; Kohzuma, T.; McFarlane, W.; Suzuki, S.; Sykes, A. G. *J. Chem. Soc., Chem. Commun.* **1994,** 581.
120. Dennison, C.; Kohzuma, T.; McFarlane, W.; Suzuki, S.; Sykes, A. G. *Inorg. Chem.* **1994,** *33,* 3299.
121. Vakoufari, E.; Wilson, K. S.; Petratos, K. *FEBS Lett.* **1994,** *347,* 203.
122. Kyritsis, P.; Dennison, C.; Ingledew, W. J.; McFarlane, W.; Sykes, A. G. *Inorg. Chem.* **1995,** *34,* 5370.
123. van de Kamp, M.; Floris, R.; Hali, F. C.; Canters, G. W. *J. Am. Chem. Soc.* **1990,** *112,* 907.
124. van de Kamp, M.; Canters, G. W.; Andrew, C. R.; Sanders-Loehr, J.; Bender, C. J.; Peisach, J. *Eur. J. Biochem.* **1993,** *218,* 229.

125. van Pouderoyen, G.; Mazumdar, S.; Hunt, N. I.; Hill, H. A. O.; Canters, G. W. *Eur. J. Biochemistry* **1994,** *222,* 583.
126. Armstrong, F. A.; Driscoll, D. C.; Hill, H. A. O. *FEBS Lett.* **1985,** *190,* 242.
127. Groeneveld, C. M.; Canters, G. W. *J. Biol. Chem.* **1988,** *263,* 167.
128. Diederix, R. E. M.; Dennison, C.; Canters, G. W. In preparation.
129. Dennison, C.; Canters, G. W. In preparation.
130. Dennison, C.; Bunning, C.; Comba, P.; Canters, G. W. Unpublished results.
131. Dennison, C.; Vijgenboom, E.; de Vries, S.; van der Oost, J.; Canters, G. W. *FEBS Lett.* **1995,** *365,* 92.
132. Dennison, C.; Berg, A.; Canters, G. W. *Biochemistry* **1997,** *36,* 3262.
133. Dennison, C.; Berg, A.; de Vries, S.; Canters, G. W. *FEBS Lett.* **1996,** *394,* 340.
134. Salgado, J.; Canters, G. W. Unpublished results.
135. Ubbink, M.; van Beeumen, J.; Canters, G. W. *J. Bacteriol.* **1992,** *174,* 3707.
136. van Spanning, R. J. M.; Wansell, C. W.; Harms, N.; Oltmann, L. F.; Stouthamer, A. H. *J. Bacteriol.* **1990,** *172,* 986.
137. Margoliash, E.; Smith, E. L.; Kriel, G.; Tuppy, H. *Nature* **1961,** *192,* 1121.
138. Ubbink, M.; Pfuhl, M.; van der Oost, J.; Berg, A.; Canters, G. W. *Protein Sci.* **1996,** *5,* 2494.
139. Benning, M. M.; Meyer, T. E.; Holden, H. M. *Arch. Biochem. Biophys.* **1994,** *310,* 460.
140. Moore, G. R.; Pettigrew, G. W. "Cytochromes *c*, Evolutionary, Structural and Physicochemical Aspects"; Springer-Verlag: Berlin, 1990.
141. Lommen, A.; Ratsma, A.; Bijlsma, N.; Canters, G. W.; van Wielink, J. E.; Frank, J.; van Beeuman, J. *Eur. J. Biochem.* **1990,** 192, 653.
142. Davis, L. A.; Schejter, A.; Hess, G. P. *J. Biol. Chem.* **1974,** *249,* 2624.
143. Ubbink, M.; Canters, G. W. *Biochemistry* **1993,** *32,* 13893.
144. Osheroff, N.; Borden, D.; Koppenol, W. H.; Margoliash, E. *J. Biol. Chem.* **1980,** *255,* 1689.
145. Ferrer, J. C.; Guillemette, J. G.; Bogumil, R.; Inglis, S. C.; Smith, M.; Mauk, A. G. *J. Am. Chem. Soc.* **1993,** *115,* 7507.
146. Ubbink, M.; Warmerdam, G. C. M.; Campos, A. P.; Teixeira, M.; Canters, G. W. *FEBS Lett.* **1994,** *351,* 100.
147. Ubbink, M.; Campos, A. P.; Teixeira, M.; Hunt, N.; Hill, H. A. O.; Canters, G. W. *Biochemistry* **1994,** *33,* 10051.
148. Martinez, S. E.; Huang, D.; Szczepaniak, A.; Cramer, W. A.; Smith, J. L. *Structure* **1994,** *2,* 95.
149. Dixon, D. W.; Hong, X.; Woehler, S. E.; Mauk, A. G.; Sishta, B. P. *J. Am. Chem. Soc.* **1990,** *112,* 1082.
150. Dixon, D. W.; Hong, X.; Woehler, S. E. *Biophys. J.* **1989,** *56,* 339.
151. Timkovich, R.; Cork, M. S.; Taylor, P. V. *Biochemistry* **1984,** *23,* 3526.
152. Timkovich, R.; Cai, M. L.; Dixon, D. W. *Biochem. Biophys. Res. Commun.* **1988,** *150,* 1044.
153. Gupta, R. K.; Koening, S. H.; Redfield, A. G. *J. Magn. Reson.* **1972,** *7,* 66.
154. Gupta, R. K. *Biochim. Biophys. Acta* **1983,** *292,* 291.
155. Senn, H.; Engster, A.; Wüthrich, K. *Biochem. Biophys. Acta* **1983,** *743,* 58.
156. Keller, R. M.; Wüthrich, K.; Pecht, I. *FEBS Lett.* **1976,** *70,* 180.
157. McIntire, W. S.; Wemmer, D. E.; Chistoserdov, A. E.; Lidstrom, M. E. *Science* **1991,** *252,* 817.
158. McIntire, W. S. *Methods Enzymol.* **1995,** *258,* 149.

159. Huizinga, E. G.; van Zanten, B. A. M.; Duine, J. A.; Jongejan, J. A.; Huitema, F.; Wilson, K. S.; Hol, W. G. J. *Biochemistry* **1992,** *31,* 9789.
160. Brooks, H. B.; Davidson, V. L. *Biochemistry* **1994,** *33,* 5696.
161. Itoh, S.; Ongino, M.; Komatsu, M.; Oshiro, Y. *J. Am. Chem. Soc.* **1992,** *114,* 7294.
162. Itoh, S.; Oshiro, Y. *Methods Enzymol.* **1995,** *258,* 164.
163. Gorren, A. C. F.; Duine, J. A. *Biochemistry* **1994,** *33,* 12202.
164. Kuusk, V.; McIntire, W. S. *J. Biol. Chem.* **1994,** *269,* 26136.
165. Gorren, A. C. F.; Moenne-Loccoz, P.; Backes, G.; de Vries, S.; Sanders-Loehr J.; Duine, J. A. *Biochemistry* **1995,** *34,* 12926.
166. Moenne-Loccoz, P.; Nakamura, N.; Itoh, S.; Fukuzumi, S.; Gorren, A. C. F.; Duine, J. A.; Sanders-Loehr J. *Biochemistry* **1996,** *35,* 4713.
167. Kenney, W. C.; McIntire, W. S. *Biochemistry* **1983,** *22,* 3858.
168. Gorren, A. C. F.; de Vries, S.; Duine, J. A. *Biochemistry* **1995,** *34,* 9748.
169. Warncke, K.; Brooks, H. B.; Babcock, G. T.; Davidson, V. L.; McCracken; J. *J. Am. Chem. Soc.* **1993,** *115,* 6464.
170. Warncke, K.; Brooks, H. B.; Lee, H.; McCracken, J.; Davidson, V. L.; Babcock; G. T. *J. Am. Chem. Soc.* **1995,** *117,* 10063.
171. Brooks, H. B.; Davidson, V. L. *J. Am. Chem. Soc.* **1994,** *116,* 11201.
172. Steinrucke, P.; Steffen, G. C.; Panskus, G.; Buse, G.; Ludwig, B. *Eur. J. Biochem.* **1987,** *167,* 431; Ciabatti, I.; Warmerdam, G. C. M.; Vijgenboom, E.; Canters, G. W. Unpublished results.
173. Ludwig, B.; Schatz, G. *Proc. Natl. Acad. Sci. U.S.A.* **1980,** *77,* 196.
174. Buse, G.; Steffens, G. C. M. *J. Bioenerg. Biomembr.* **1991,** *23,* 269.
175. Hartmann, C.; Klinman, J. P. *J. Biol. Chem.* **1987,** *262,* 962.
176. Bishop, G. R.; Davidson, V. L. *Biochemistry* **1995,** *34,* 12082.
177. Bishop, G. R.; Brooks, H. B.; Davidson, V. L. *Biochemistry* **1996,** *35,* 8948.
178. Bishop, G. R.; Valente, E. J.; Whitehead, T. L.; Brown, K. L.; Hicks, R. P.; Davidson, V. L. *J. Am. Chem. Soc.* **1996,** *118,* 12868.
179. Brooks, H. B.; Jones, L. H.; Davidson, V. L. *Biochemistry* **1993,** *32,* 2725.
180. Davidson, V. L.; Jones, L. H.; Graichen, M. E. *Biochemistry* **1992,** *31,* 3385.
181. Hyun, Y.-L.; Davidson, V. L. *Biochim. Biophys. Acta* **1995,** *1251,* 198.
182. (a) Ubbink, M.; Hunt, N. I.; Hill, H. A. O.; Canters, G. W. *Eur. J. Biochem.* **1994,** *222,* 561; (b) Kyritsis, P.; Kohzuma, T.; Sykes, A. G. *Biochim. Biophys. Acta* **1996,** *1295,* 245.
183. Gorren, A. C. F.; van der Palen, C. J. N. M.; van Spanning, R. J. M.; Duine, J. A. In "Microbial Growth on C1 Compounds"; Lidstrom, M. E., and Tabita, F. R., Eds.; Kluwer Academic: Dordrecht, The Netherlands, 1996; pp. 197–204.
184. Gray, K. A.; Davidson, V. L.; Knaff, D. B. *J. Biol. Chem.* **1988,** *263,* 13987.
185. Davidson, V. L.; Jones, L. H. *J. Biol. Chem.* **1995,** *270,* 23941.
186. Davidson, V. L.; Jones, L. H. *Biochemistry* **1996,** *35,* 8120.
187. Lappalainen, P.; Watmough, N. J.; Greenwood, C.; Saraste, M. *Biochemistry* **1995,** *34,* 5824.
188. Davidson, V. L.; Graichen, M. E.; Jones, L. H. *Biochim. Biophys. Acta* **1993,** *1144,* 39.
189. Merli, A.; Brodersen, D. E.; Morini, B.; Chen, Z.; Durley, R. C. E.; Mathews, F. S.; Davidson, V. L.; Rossi, G. L. *J. Biol. Chem.* **1996,** *271,* 9177.
190. Gray, K. A.; Knaff, D. B.; Husain, M.; Davidson, V. L. *FEBS Lett.* **1986,** *207,* 239.
191. Witt, H.; Zichermann, V.; Ludwig, B. *Biochim. Biophys. Acta* **1995,** *1230,* 74.